Ice injected up to the Tropopause by Deep Convection: 1) in the Austral Convective Tropics

Iris-Amata DION[1], Philippe RICAUD[1], Peter HAYNES[2], Fabien CARMINATI[3] and Thibaut DAUHUT[4]

[1] CRNM, Meteo-France - CNRS, Toulouse, 31057, France

5   [2] DAMTP, University of Cambridge, Cambridge, CB3 0WA, United Kingdom

[3] Met Office, Exeter Devon EX1 3PB, United Kingdom

[4] Laboratoire d'Aerologie, Université de Toulouse, CNRS, UPS, Toulouse, 31400, France

Correspondence to: Iris-Amata DION (iris.dion@meteo.fr)

Abstract. The contribution of deep convection to the amount of water vapour and ice in the Tropical Tropopause Layer

10   (TTL) from the tropical upper troposphere (UT, around 146hPa) to the Tropopause Level (TL, around 100hPa) is investigated. Ice water content (IWC) and water vapour (WV) measured in the UT and the TL by the Microwave Limb Sounder (MLS, Version 4.2) are compared to the precipitation (Prec) measured by the Tropical Rainfall Measurement Mission (TRMM, Version 007). The two datasets, gridded within $2° \times 2°$ horizontal bins, have been analyzed during the austral convective season: December, January and February (DJF) from 2004 to 2017. MLS observations are performed at

15   01:30 and 13:30 Local Solar Time whilst the Prec dataset is constructed with a time resolution of 1 hour. The new contribution of this study is to provide a much more detailed picture of the diurnal variation of ice than is provided by the very limited (2 per day) MLS observations. Firstly, we show that IWC represents 70 and 50% of the total water in the tropical UT and TL, respectively and that Prec is spatially highly correlated with IWC in the UT (Pearson linear coefficient R=0.7). We propose a method that uses Prec as a proxy of deep convection bringing ice up to the UT and TL during the

20   growing stage of the convection, in order to estimate the amount of ice injected in the UT and the TL, respectively. We validate the method using ice measurements from the Superconducting Submillimeter-Wave Limb-Emission Sounder (SMILES) during the period DJF 2009-2010. Next, the diurnal cycle of injection of IWC into the UT and the TL by deep convection is calculated by the difference between the maximum and the minimum in the estimated diurnal cycle of IWC in these layers and over selected convective zones. Six tropical highly convective zones have been chosen: South America,

25   South Africa, Pacific Ocean, Indian Ocean, and the Maritime Continent region, split into land (MariCont-L) and ocean (MariCont-O). IWC injection is found to be 2.73 and 0.41 mg m^{-3} over tropical land in the UT and TL, respectively, and 0.60 and 0.13 mg m^{-3} over tropical ocean in the UT and TL, respectively. The MariCont-L region has the greatest ice injection in both UT and TL (3.34 and 0.42-0.56 mg m^{-3}, respectively). The MariCont-O region has less ice injection than MariCont-L (0.91 mg m^{-3} in the UT and 0.16-0.34 mg m^{-3} in TL), but has the highest diurnal minimum value of IWC in the

30   TL (0.34-0.37 mg m^{-3}) among all oceanic zones.

1 Introduction

Water vapour (WV) is one of the main greenhouse gases and has an important impact on the climate, particularly in the tropics. WV concentrations are limited by temperature which regulate the saturation mixing ratio in air masses (Hartmann et al., 2001; Fueglistaler et al., 2009; Khaykin et al., 2013). In consequence, WV is much smaller in the upper troposphere (UT) and stratosphere than in the lower troposphere. However, despite the small concentrations, the WV distribution in the tropical upper troposphere (e.g. Soden et al., 2008) and stratosphere (e.g. Solomon et al., 2010) plays an important role on climate, including the determination of the overall radiative balance of the troposphere. The WV distribution in this region of the atmosphere is strongly coupled to the distribution of cirrus clouds which despite being thin, can have a significant effect on the overall thermal balance of the troposphere (e.g. Zhou et al., 2014). The tropical upper stratosphere and lower stratosphere recognized as a distinct region of the atmosphere – the Tropical Tropopause Layer (TTL) – is defined by the layer between the level of maximum convective outflow (10-12 km, ~200 hPa) that closely corresponds to a minimum in ozone and the cold point temperature (CPT) (16-17 km, ~100 hPa) (Gettelman and Forster, 2002; Mehta et al., 2008; Birner and Charlesworth, 2017). Within the TTL, a complex set of physical processes interact to determine the distribution of temperature, WV and clouds, and other radiatively active chemical species (e.g. Fueglistaler et al., 2009; Randel and Jensen, 2013). The TTL is important in determining several aspects of troposphere-to-stratosphere exchange and therefore determining the chemical composition of the stratosphere. Much attention has therefore been focused on the role of TTL processes in setting the value of WV concentrations that enter the stratosphere. In particular, there has been an ongoing debate of the relative important of large-scale processes in which air masses move slowly from troposphere to stratosphere within the large-scale three-dimensional circulation and dehydrates as it encounters very cold temperatures and small-scale processes, in which convection injects WV (and ice) directly into the TTL and, the stratosphere, with potentially hydrating impact. The relative importance of the three-dimensional circulation processes and convective processes continues to be debated (e.g. Alcala and Dessler, 2002; Liu and Zipser, 2005; Carminati et al., 2014).

For intense, Ueyama et al. (2015) have shown that tropical waves dehydrate the TTL by 0.5 ppmv while the cloud microphysical processes and convection moisten the TTL by 0.7 and 0.3 ppmv, respectively. Some authors have shown that fast overshoots from deep convection transports very rapidly water upward (from few minutes to one hour) into the stratosphere (Pommereau et al., 2010; Dauhut et al., 2015). Liu and Zipser (2005) have found that 1.3% of tropical convection systems reach 14 km and 0.1% of them may even penetrate the 380 K potential temperature level which corresponds to the CPT. Avery et al. (2017) have also suggested that tropical convective ice cloud and associated cirrus sublimating at unusually high altitudes might also have a role in stratospheric hydration. The other path for water entrering the lower stratosphere (LS) is the slow vertical advection (300 m month^{-1}) governed by radiative heating (Holton and Gettelman, 2001; Gettelman and Forster, 2002; Corti et al., 2006; Fueglistaler et al., 2009). Once into the UT or the TTL, the amount of the relative humidity of the layer impacts the ice nucleation, growth and sedimentation (Peter et al., 2006).

Whilst there is observational evidence for convective hydration events (Liu and Zipser, 2005; Pommereau et al., 2010; Avery et al., 2017) and convective hydration of the stratosphere has been clearly corroborated by state-of-the-art numerical simulations (e.g. Dauhut et al., 2015), the quantitative role of convective hydration in determining water vapour concentrations in the main body of the stratosphere remains uncertain. One approach has been to combine observational estimates of overshooting convection frequency with information from short-localised duration numerical simulations. Using this approach, Dauhut et al. (2015) have estimated that 18% of the water mass flux across the 380 K potential temperature level is due to overshooting deep convection. Another has been to include estimates of convective penetration, e.g. from satellite observations into large-scale trajectory calculations. The conclusions are sensitive to the assumptions made but, for example, Wright et al. (2013) and Schoeberl et al. (2018), both conclude that the effect of convective penetration on WV concentrations in the stratosphere is very weak, essentially because most air masses that are moistened by convective injection are subsequently dehydrated during encounter cold temperatures on the large-scale before they reach the main body of the stratosphere.

Whether or not convective processes play a direct role in determining stratospheric WV concentrations, it is clear that, moving from the lower TTL to the upper TTL, convective-scale processes play an increasingly important role in determining the distributions of WV and of cirrus. Representing convective-scale processes in global models used for weather climate prediction is challenging, and it is important where possible to evaluate model representations by finding observed characteristics of WV and cirrus in the TTL that can be usefully compared to model simulations. One opportunity is provided by diurnal variations. The time scale is of course very different to the decadal and longer timescales of interest in climate prediction, but the short time scale has the advantage of providing time series with many cycles which is therefore well characterised statistically. The diurnal cycle is one of the most fundamental modes of variability of the global climate system and is associated with large and well-defined variations in the solar forcing (Yang and Slingo, 2001). The amplitude of the surface thermal diurnal cycles in the tropics is ten times stronger than the amplitude of the surface thermal annual cycle (Beucher, 2010) and the diurnal cycle of deep convection is mainly governed by the surface thermal diurnal cycle. Understanding the diurnal cycle of the total water in the tropical UT, TTL and LS contributes to characterize the total water exchange between the UT and the LS in the tropics. Many studies (e.g. Jiang et al., 2014) have shown that the diurnal cycle of ice in the UT is linked to the diurnal cycle of the convection. The maximum of deep convection in the UT has been shown to peak in the local afternoon over land and in the local early morning over ocean (Liu and Zipser, 2005). Based on these studies and with data from the space-borne Microwave Limb Sounder (MLS) instrument, Carminati et al. (2014) studied the diurnal cycle of WV and ice in the TTL over Africa and South America and have shown the presence of a strong diurnal signal over the two continents. Suneeth et al. (2017) have shown the differences in the diurnal cycles of CPT altitudes and CPT temperatures over tropical land and ocean. The diurnal cycle of temperature has also been studied in the TTL (Khaykin et al., 2013) showing that the amplitude of temperature anomalies increases with the intensity of the convection.

In summary, the processes driving the total water diurnal cycle are different in the UT and at the tropopause layer, e.g. only the deepest convection directly impacts water content at the tropopause layer and saturation is more frequent at the

tropopause layer than in the UT. Since the total water diurnal cycle in the tropopause layer is still not well described in global models (Jiang et al., 2014), space-borne observations may improve our understanding of the processes occurring in this layer. This provides motivation for the study presented in this paper, in which we consider the diurnal cycle of ice in the
100 TTL, for which limited, but nonetheless valuable data is provided by the MLS instrument.

The aim of the present study is to quantify the role of the deep convection on the hydration and dehydration of the TTL. For that, we focus on the diurnal injection of ice in the tropical UT and the tropopause layer from the deep convective activity and address the question relative to the diurnal cycle of total water over tropical deep convective areas.

Africa and South America are two land regions of intense deep convective activity in the tropics, together with the Maritime
105 Continent region (MariCont, the region made of lands and oceans, between the Indian Ocean and the West Pacific, presented by the red box in Fig. 1). However, the deep convective systems occur more frequently and strongly over the MariCont region (Liu and Zipser, 2015) than over the other continental zones. It is known that excess of energy received by tropical surfaces is mainly balanced and transferred over land by convection toward mid-latitudes and over ocean by both convection and oceanic circulation. However, over the MariCont region, seas and oceans currents transferring energy toward mid-
110 latitudes are slowed down and blocked by the thousands of islands. Consequently, the excess of energy in the oceanic surface over the MariCont region is mainly balanced by transfer from convection. The diurnal cycle of WV and ice has already been studied over Africa and South America and over the whole tropical band (see e.g. Liu and Zipser, 2009; Millán et al., 2013; Carminati et al., 2014). The MariCont region is the driest and coldest area at the CPT and the water budget in the TTL over the MariCont region separating MariCont land and MariCont ocean is still unknown. Furthermore the physical mechanism
115 governing the diurnal cycle of convection and surface precipitation over ocean is still an open question.

In order to understand the total water diurnal cycle up to the TTL, we first use 13 years of the ice water content (IWC) and WV measurements from MLS (Version 4.2x) and surface precipitations (Prec) from the TRMM instrument. Then, we use WV, IWC, total water ($\sum W = WV + IWC$), relative humidity with respect to ice (RHI) and temperature (TEMP) from MLS and Prec from TRMM over the period 2004 to 2017 in order to better understand the water fraction (IWC/$\sum W$) in the UT
120 (~146 hPa) and the tropopause layer (TL, ~100 hPa, around the CPT). The relationships between surface precipitation and the processes in the UT and the TL are investigated. Our study intends to evaluate the mechanisms affecting the diurnal cycle of total water in the TL above land and ocean with a particular emphasis over the MariCont region due to its topographical complexity. Thus, the diurnal cycle of ice (provided by MLS but with very poor time resolution) is improved and better understood thanks to the relation with the diurnal cycle of precipitation (provided by TRMM with a much better time
125 resolution).

The main instruments used are presented in Section 2. The methodology developed to establish the link between the diurnal cycle of surface processes and the diurnal cycle of water in the UT and TL is presented in Section 3. The estimated diurnal injection of IWC in the UT and TL from deep convective activity is presented in Section 4. Finally, the influence of the convective dissipating stage on the decreasing phase of the IWC diurnal cycle in the UT and the TL is discussed in Section 5

130 and conclusion will be drawn in Section 6. This paper contains many abbreviations and acronyms. To facilitate reading, we compile them in the Appendix.

2 Instruments

2.1 MLS

MLS is a microwave instrument aboard the NASA's Earth Observing System (EOS) Aura platform (Livesey et al., 2017), measuring in a limb viewing geometry to maximize signal intensities and vertical resolution. The MLS instrument is aboard a sun-synchronous near-polar orbiter completing 233 revolution cycles every 16 days giving a daily global coverage with

140 about 14 orbits. Aura is crossing the equator at 01:30 local time (LT) and 13:30 LT. Among all the atmospheric parameters measured by MLS, we focus on: IWC, WV, TEMP and RHI. Although IWC (mg m^{-3}) is valid between 215 and 82 hPa, the number of scientifically-exploitable measurements at 82 hPa within a 2°x2° pixel is not significant. In our study, we will only use two levels to analyse IWC, at 180 and 100 hPa. WV (ppmv) is valid between 316 and 0.002 hPa, TEMP (K) between 261 and 0.001 hPa and RHI (%) between 1000-1.0 hPa. The MLS IWC sensitivity thresholds are 0.1 mg m^{-3} in the

145 UT and 0.02 mg m^{-3} in the TL (Livesey et al., 2017) and will imply an under-estimation of the IWC measured values.

 The MLS v4.2x data processing validated by Livesey et al. (2017) presents significant and minor differences with the previous MLS version. The total random noise in v4.2x IWC is larger than the one in v2.2. Compared with the v3.3 of MLS (used for instance in Carminati et al., 2014), the v4.2 improves IWC composition profiles in cloudy regions especially in the upper troposphere over the tropics and improves the WV at global scale (Livesey et al., 2017).

150 Level 2 data quality tests (filter and data screening) from the v4.2x have been applied to WV, IWC, RHI, and TEMP as suggested by Livesey et al. (2017). The MLS measurements estimated from the averaging kernels (Livesey et al., 2017) are used to characterize the distribution of the four parameters on two layers: one at 146 hPa (UT) and one at 100 hPa (TL). The vertical resolution of the IWC measurements is ~3 km, the horizontal resolution is ~300 km and 7 km along and across the track, respectively. The WV vertical resolution is 2.5 ± 1.2 km and the WV along track horizontal resolution is between 170

155 and 350 km. The TEMP vertical resolution is 4.5 km.

In the study of Carminati et al. (2014), a 10°×10° resolution was chosen with seven years of MLS data processed with version 3.3 (v.3.3). In our study, MLS data have been averaged over a much longer period (2004 to 2017) in a much higher horizontal resolution of 2°×2° (~200×200 km). In each 2°×2° bin, and for the 13 years average, any bin with less than 60 measurements in the daytime (Day at 13:30 LT) or the nighttime (Night at 01:30 LT) datasets is excluded in order to have

160 significant statistics. Thus, the maximum of measurements per bin during the 13 years period is ~ 470 and the minimum is fixed to be 60. The number of measurements over the MariCont region is on average the lowest over the tropics. Consistent

with Carminati et al. (2014) and Liu and Zipser (2005), we use the difference between the MLS measurements performed during the Day and the Night to study the "Day minus Night" (Day−Night) signal.

2.2 TRMM

The TRMM satellite was launched in November 1997 (https://trmm.gsfc.nasa.gov/publications_dir/publications.html). TRMM carried 5 instruments: a 3-sensor rainfall suite, the precipitation radar, the TRMM Microwave Imager, the Visible and Infrared Scanner and 2 related instruments, the Lightning Imaging Sensor and the Clouds and the Earth's Radiant Energy System. In our study, we use the Algorithm 3B42 producing the TRMM merged high quality to infrared precipitation and root-mean-square precipitation-error estimation with the TRMM version 007. The rainfall level 3 measurements (mm hr^{-1}) are vertically integrated precipitation (Prec). TRMM Prec data are provided in the tropics within a 0.25°×0.25° horizontal resolution extending from 50°S to 50°N. TRMM datasets used in our study in coincidence with the MLS period of measurements from 2004 to 2017. In order to compare to the MLS measurement, we degraded the TRMM resolution to 2°×2° in averaging the TRMM measurements in each box of 2°x2° of MLS. Furthermore, as TRMM follows an orbit precession, shifting few minutes per day, the 24-hour diurnal cycle can be averaged over the period of study, with 1-hour resolution over the 24 hour diurnal cycle.

2.3 SMILES

The Superconducting Submillimeter-Wave Limb-Emission Sounder (SMILES) was a Japanese atmospheric limb sounding instrument on board the International Space Station (ISS) platform. SMILES measurements of ice are used in this study. The instrument measured IWC between 120 and 80 hPa and the measurement of tropospheric ice, the partial Ice Water Path (pIWP) integrated between 1000 and 180 hPa, during the short period of October 2009 to April 2010. As ISS follows a low Earth orbit, with about 15 orbits a day, the ice measurements in the troposphere and tropopause layer over the entire 40°N-40°S band can be provided in about two months. Thus, the austral convective season of DJF is enough to covers the entire tropical band. Furthermore, as each orbit is drifted about 20 min earlier each day, the entire diurnal cycle of ice can be provided during this period. In the present study, SMILES measurements will be used as reference of diurnal cycle of ice and will be compared to the climatology of the diurnal cycle of ice estimated in the UT and the TL.

3 Relationship between Prec and water budget in the austral convective UT and TL

In this section, we analyse the relationships between Prec and the water budget in the UT and the TL during the DJF season, highly convective season of the southern hemisphere. Deep convection can affect water vapour and ice in the UT and the TL whereas Prec measurements include the contribution of both shallow convection (that does not reach the UT) and deep convection (reaching the UT and the TL).

3.1 Tropical distribution of Prec and water budget in the UT and TL

The daily averaged ((D+N)/2) Prec measured by TRMM at the resolution of 0.25°×0.25° and 2°×2° (the same horizontal resolution as MLS) are shown in Figures 1a and b, respectively. The fine structure of the horizontal distribution of Prec at the high resolution (0.25×0.25°) over South Africa, South America, Western Pacific Ocean and the Maritime Continent are degraded when considering Prec at low resolution (2°×2°). Figure 1c presents the Local Solar Time (evaluated for each bin of 0.25°×0.25°) at which the diurnal cycle of Prec reaches its maximum in TRMM observations showing the large variability and complexity of the diurnal maximum of Prec over the tropics. The daily averages of IWC, WV, IWC fraction (IWC/$\sum$W), TEMP and RHI from MLS in the tropics are shown in Figure 2 for the UT (at 146 hPa) and Figure 3 for the TL (100 hPa).

In DJF, local maxima of Prec (Fig. 1), IWC, WV, IWC fraction and RHI in the UT (Fig. 2) are found over the main convective areas: South America, South Africa, MariCont, North of Australia, along the Inter-Tropical Convergence Zone (ITCZ) and the South Pacific Convergence Zone (SPCZ). Maximum values of Prec, IWC, WV and RHI over the whole tropics are located over the MariCont (and North Australia) (Figs. 1a and b and Figs. 2a, b, c and e). Minima of Prec, IWC, WV, IWC fraction and RHI are found over Eastern Pacific Ocean and South Atlantic Ocean. Over MariCont region, we observe the maximum of tropical IWC and the minimum of temperature (Figs. 2a and d). The IWC fraction shows that, over the region of high Prec (> 0.20 mm h^{-1}), up to 70% of the $\sum$W is composed of ice. The RHI is higher over land than over ocean but RHI never exceeds 100% at 146 hPa, on average at 2°x2° resolution (consistently with the RHI tropical vertical profil shown by Fueglistaler et al., 2009). The MariCont region exhibits the highest RHI with values close to 100%. In summary, there is a strong spatial link between Prec and water (IWC and WV) in the UT.

In the TL (Fig. 3), IWC is lower than in the UT (~3 mg m^{-3} at 146 hPa vs < 1 mg m^{-3} at 100 hPa) but the horizontal distribution of IWC is correlated with the horizontal distribution of Prec and shows maxima over South America, South Africa, the MariCont region and Western Pacific Ocean. The main difference between the UT and the TL is the minimum of WV observed over the MariCont region (> 8 ppmv at 146 hPa and < 3 ppmv at 100 hPa). With the decrease of temperature from the UT to the TL (Figs. 2 and 3) and the associated decrease of WV at saturation, the observed WV decreases by more than 11 ppmv over the MariCont region and by around 5 ppmv in other regions. In the TL, the IWC and the fraction of water in the ice form is larger over MariCont (beyond 1 mg m-3 and near 78%, respectively) than elsewhere in the tropics. RHI in the TL reaches high values (RHI ~100 %) highlighting a saturated environment over the central South America, Africa, East of MariCont and the Western Pacific Ocean. In comparison to other tropical regions, the larger IWC over the MariCont can be explained by (i) the larger condensation of water vapour associated with the larger temperature drop from the UT to the TL, and (ii) a larger transport of ice into the TL by deep convection.

To investigate the vertical distribution and the diurnal cycles of water species in the TL, we have defined, from results presented Fig.1–3, seven tropical convective zones shown in Figure 4: South America (SouthAm, 0°N-30°S), South Africa (SouthAfr, 0°N-30°S), Pacific Ocean (PacOc, 0°N-30°S; 180°W-150°W), Indian Ocean (IndOc, 0°N-30°S; 60°E-90°E), MariCont (10°N-15°S; 90°E-160°E), MariCont land (MariCont-L) and MariCont ocean (MariCont-O). Land and ocean over

225 the study zones have been separated using the Solar Radiation Data (SoDa, http://www.soda-pro.com/web-services/altitude/srtm-in-a-tile), providing a TIFF image with values from the Shuttle Radar Topography Mission (SRTM) Digital Elevation Model. Each zone is defined at a horizontal resolution of 2°x2°.

3.2 Water budget in the UT and the TL

230 To investigate the processes in the UT and TL which drive the water budget, the vertical profiles of TEMP, WV, IWC and RHI are shown for the different study zones in Figure 5. To complete the comparison between the study zones, the DJF average of the tropopause pressure level is represented over all the tropics in Figure 6 from the National Centers For Environmental Prediction (NCEP).

In Fig. 5a, the tropical CPT is found between 100 and 80 hPa consistently with previous results presented in e.g. Fueglistaler

235 et al. (2009) and Kim and Son (2012). The tropical tropopause defined by NCEP (Fig. 6) is close to the level given by MLS at 100 hPa we named the TL in this study (~ 100-115 hPa). Furthermore, the tropopause pressure shown in Fig.6 is lower (higher altitude) over ocean than over land. While the pressure at the tropopause over West Pacific, South Arabia, Caribbean sea present is the lowest (~105 hPa). Furthermore, the tropopause is the coldest (Fig. 5a) and has the highest pressure (lower altitude) (Fig. 6) over the MariCont. Regarding WV, the tropical UT is more humid than the TL: the decrease from the UT at

240 146 hPa to the TL at 100 hPa is about 7 ppmv for WV, and 1 mg m^{-3} for IWC (the two dashed lines in Figs. 5b and c, respectively). These results are consistent with previous studies all presented in Fueglistaler et al. (2009).

RHI is lower in the UT than at the TL by ~10 % (Fueglistaler et al., 2009) (Figs. 2d and 3d, respectively). Since the UT is on average sub-saturated, convective-lifted ice can sublimate and can be seen as a source of WV. At the TL, as the atmosphere is in average close to saturation (RHI ~100%) over SouthAm, SouthAfr, MariCont and the Western Pacific Ocean (Fig. 3), the

245 convective-lifted ice is statistically more often transported into a saturated or supersaturated region. In such context, the associated ice hydrometeors grow and sediment, and can also be transported down by convective downdrafts. These processes contribute to the loss of ice in this layer. Furthermore, the TL is the level of greatest dehydration because of supersaturation with respect to ice (Jensen et al., 1996; Jensen et al., 2005). In supersaturation conditions, the excess of water vapour can condensate on existing ice crystals (or form new ones in presence of condensation nucleus) allowing ice crystals

250 to grow and sediment which dehydrates the layer. Conversely, hydration may occur in the LS (if reached by convection) because this layer is subsaturated with respect to ice (Khaykin et al., 2009; Allison et al., 2018; Dauhut et al, 2018).

3.3 Spatial correlation between Prec and water in the UT

This section presents the relationship between deep convection and the water vapour and ice injected in the UT. We have

255 calculated the Pearson linear correlation coefficient R between the horizontal distribution of Prec and both IWC and WV at 146 hPa during the Day, the Night and the Day-Night over the study zones (see Table 1). We denote Prec, IWC and WV at

146 hPa during Day, Night and Day-Night, by $Prec_x$, IWC_x^{146} and WV_x^{146}, respectively (where x= Day, Night or Day−Night). The spatial correlation between IWC and Prec is defined by the following equation:

$$IWC_x^{146} = \alpha_x \times Prec_x + \beta_x \qquad (1)$$

260   where α_x is the regression coefficient and β_x is the offset.

The spatial correlation for the 6 zones is shown in Table 1. The spatial correlation of IWC_{Day}^{146} and IWC_{Night}^{146} with Prec is high ($R \sim 0.7$-0.9) over SouthAm, SouthAfr, PacOc and IndOc and smaller ($R \sim 0.5 - 0.6$) over the MariCont region (MariCont-L, MariCont-O and MariCont). The spatial inhomogeneity of the MariCont surface with thousands of islands, seas and coastal areas may probably explain the lower space correlation between the Prec and IWC[146]. The regression coefficient between

265   $Prec_x$ and IWC_x (Table 1) α_x, can be interpreted as the efficiency of the convective system to inject ice in the UT. Comparing α_x in Day and Night conditions, SouthAfr, SouthAm, MariCont-L, MariCont-O and MariCont stand out with larger Day values ($\alpha_D = 7.5$-15.0 mg m^{-3} mm^{-1} h) than IndOc and PacOc or than Night values ($\alpha_x = 4.7$-7.7 mg m^{-3} mm^{-1} h). Over land, all regions under consideration show a better efficiency to inject ice in the UT during Day than during Night. β_x is considered as the IWC background. Over land and ocean regions, β_x is close to zero. β_{Day} is the highest over the MariCont-

270   L (1.1 mg m^{-3}) and null over SouthAm (0.0 mg m^{-3}). Over the oceans, there is no significant differences between β_{Day} and β_{Night} for the injected ice in the UT, except over PacOc.

Following Liu and Zipser (2009) and Carminati et al. (2014), we also study the difference between Day and Night, to obtain information on the IWC^{146} diurnal cycle. Figure 7 shows the $Prec_{Day-Night}$, $IWC_{Day-Night}^{146}$ and $WV_{Day-Night}^{146}$, respectively. Convective regions such as SouthAm, SouthAfr, even along the ITCZ, are characterized by a positive Day−Night signal in

275   $Prec_{Day-Night}$ and IWC_x^{146} with values greater than 0.10 mm hr^{-1} and 0.20 mg m^{-3}, respectively (Figs. 7a and b). The spatial correlation R between $Prec_{Day-Night}$, and $IWC_{Day-Night}^{146}$ is greater over the 3 land zones ($R \geq 0.6$-0.7) than over the 3 ocean zones ($R \leq 0.1$-0.5). MariCont-O region shows the highest oceanic correlation ($R \sim 0.5$) compared to the PacOc and IndOc regions ($R = 0.2$ and 0.1, respectively). The low R values over IndOc and PacOc could be explained by: i) the low $IWC_{Day-Night}$ variability compared to the high $Prec_{Day-Night}$ variability observed over ocean and ii) the low amplitude of the

280   deep convection diurnal cycle over ocean (Liu and Zipser, 2005). We could hypothesize that IWC^{146} over the MariCont-O is more influenced by local deep convection than over IndOc and PacOc. However, considering IWC^{146} and Prec during Day and Night independently, we find good correlation over the ocean (~ 0.6-0.8 mg m^{-3}).

The spatial correlation R between $Prec_x$ and WV_x^{146} remains low in all configurations, with values of 0.-0.5 (Table 1). The spatial correlation between the $WV_{Day-Night}^{146}$ and $Prec_{Day-Night}$ shows an average over the 7 study zones of $\mu_{Zones} \sim 0.07$ with

285   small negative correlations over SouthAm and SouthAfr and with a regression coefficient α_x between WV^{146} and Prec calculated to be $\alpha_x = 0$ (Table 1). We conclude that WV is not spatially correlated with the diurnal cycle of the deep convection. These results are consistent with results from Liu and Zipser (2009) and Carminati et al. (2014) showing that the

Day−Night signal of WV measured by MLS is very different with the Day−Night signal of IWC measured by MLS in the UT over land.

290 Deep convection does not inject directly WV in the UT, but injects ice which then may sublimate into WV. Modelling studies with Cloud Resolving Models illustrate the sequence of mecanisms (ice uplift, mixing, sublimation) that leads convection to hydrate initially subsaturated layers (Dauhut et al., 2015, 2018, and Lee et al., 2018). In Dauhut et al. (2015), the onset of the WV increase is delayed by 1-3 hours with respect to the onset of deep convection (~12:00 LT). Such delay can explain why $WV^{146}_{Day, Night}$ and $Prec_{Day, Night}$ are not spatially correlated in observations ($R \sim 0.2$), while the space correlation R between

295 $IWC^{146}_{Day,Night}$ and $Prec_{Day, Night}$ is stronger ($R \sim 0.7$). For this reason, we now focus on the diurnal cycle of ice and on the amount of ice injected in the UT and the TL by deep convective systems traced by Prec.

3.4 Diurnal cycle of Prec

This section is presenting the diurnal cycle of Prec over the 6 study zones during the Southern Hemisphere convective

300 season (DJF) from 2004 to 2017 over land and ocean, respectively (Figures 8a and b).

Over land, the amplitude (peak to peak) of the Prec diurnal cycle varies between 0.2 and 0.3 mm h^{-1}, with simultaneous minima between 08:00 and 09:00 LT within the regions. MariCont-L area shows the driest minimum (0.09 mm h^{-1}) and the wettest and latest maximum (16:00-17:00 LT, 0.385 mm h^{-1}). SouthAm and SouthAfr maxima are found at 14:00-15:00 LT and 15:00-16:00 LT, respectively.

305 Over ocean, the amplitude of the Prec diurnal cycle varies between 0.08 and 0.1 mm h^{-1}, with simultaneous minima between 17:00 and 18:00 LT. However, the maxima are spread between 01:00 and 06:00 LT.

The main difference between Prec diurnal cycle over tropical ocean and land are: i) morning maximum over ocean compared to early afternoon over land, ii) peak to peak diurnal cycle of Prec is larger over land than over ocean and iii) minima can be twice lower over land (0.1 mm h^{-1}) than over ocean. The comparison of the Prec diurnal cycle over MariCont and MariCont-

310 O or MariCont-L highlights the importance of analyzing separately the diurnal cycle over land and over ocean in this region, because MariCont-O and MariCont-L have two distinct behaviours which are hidden when the diurnal cycle is only considered over the MariCont global area.

3.5 Time correlation between Prec and IWC during the growing convective phase in the UT

315 In this section, we quantify the link between deep convection reaching the UT and Prec. The diurnal cycle of Prec is compared to the diurnal cycle of the frequency of overshooting precipitation features (OPFs) events (i.e. the proportion of all OPF events that occurs in various ranges of time of day, adapted from Figure 3 of Liu and Zipser (2005) from global satellite radar measurements) over land (Figure 9a) and ocean (Figure 9b) in the tropical band (20°S-20°N). The OPFs considered by Liu and Zipser (2005) are tropical deep convective systems penetrating the tropical TL (called $Z_{tropopause}$ in Liu and Zipser

320 (2005)). The OPFs are calculated from measurements from January 1998 to November 2000 and from December 2001 to

December 2003 based on TRMM precipitation radar (PR) measured reflectivity into precipitation features (PFs) and using the method described by Nesbitt et al. (2000). The OPFs can be identified thanks to the high vertical resolution of the TRMM PR.

Over land, the diurnal cycle of Prec and OPF shows a maximum at 16:00-17:00 LT and a minimum at 09:00-10:00 LT (Fig. 9a). The duration of the growing phase, defined as the period between the minimum and the maximum of Prec, is the same for OPF and Prec, and lasts $\Delta t = 7$ hours. The major difference in the diurnal cycles of Prec and OPF occurs after the growing phase: the fraction of OPF decreases more rapidly than that of Prec and stops decreasing around 00:00 LT whereas that of Prec continues to decrease. This difference can be explained by the contribution to Prec of 1) the convection that does not reach the stratosphere and 2) the mature phase of the OPF that produces stratiform rain for some hours after the overshooting time. These results over land are consistent with Pereira et al. (2006) showing that the shallow convection is associated with 10% of precipitation over Amazonian region. Although OPF and Prec diurnal cycles are not calculated over the same study period, we can deduce from the present analysis that during the growing phase, the time evolution of Prec is a good proxy for the time evolution of deep convection reaching the TL (OPFs).

Over ocean, the sea surface temperature (SST) does not have a strong diurnal cycle (less than ~1 K) with a peak in the early afternoon (e.g., Chen and Houze, 1997; Stuart-Menteth et al., 2003). The convective clouds usually develop after the SST peak, during the afternoon and during the night with a maximum in the early local morning. The diurnal cycle of Prec and OPF (Fig. 9b) over the ocean have a maximum over night (05:00-06:00 LT) and a minimum in the end of the afternoon (18:00-19:00 LT for the OPF and 20:00-21:00 LT for the Prec). The diurnal cycles of OPF and Prec over the ocean show similar amplitudes in deviation from the mean. This result is consistent with Peirera et al. (2005) showing that the shallow convection is associated with only 3% of precipitation over Eastern Pacific region.

In summary, although OPFs are representative of deep convection reaching the TL, OPFs developped and presented in Liu and Zipser (2005) are not available during our study period of 2004-2017. However, our results in this section have shown that during the growing stage of deep convection, Prec is a good proxy of convection reaching the TL over land and ocean. Thus, as Prec is available in time coincidence with MLS IWC ans WV over 2004-2017, we will use Prec to interpret the time evolution of IWC in the UT and the TL.

4. Amount of ice injected in the UT and the TL by deep convection

In this section, we present the method we have developed to estimate the diurnal cycle of IWC in the UT $\left(IWC^{UT}(t)\right)$ and in the TL $\left(IWC^{TL}(t)\right)$ based on the diurnal cycle of Prec and on the two per day IWC measurements by MLS. Like in the previous section for OPF, we separate the diurnal cycle of IWC into a growing phase (period when deep convection develops to reach the UT and the TL), and a decreasing phase (period when deep convection dissipates). During the growing phase, Prec is a good indicator (proxy) of deep convection both over land and ocean (section 3.5). This is not true during the

decreasing phase, when shallow convection can have a significant impact on Prec. Since IWC is spatially highly correlated

355   with Prec and since the deep convection (OPFs) bringing ice into the TL increases with Prec during the growing phase, we

expect ice to be injected up to the UT and the TL with a delay $\left(\delta t^{UT,TL}\right)$ after the onset of the deep convection t_{on} during the

growing phase.

The method developed focuses on the growing stage of deep convection. We quantify the amount of ice injected to the UT

and the TL and determine the onset time of the ice injection and its duration. The amount of ice injected will be calculated

360   from the estimation of the amplitude of the diurnal cycle of IWC in the UT and the TL.

4.1 IWC diurnal cycle in the UT and TL

The method to estimate $IWC^B(t)$ *(B = UT or TL)* is presented in this section. Figure 10 illustrates the methodology to find

the $IWC^B(t)$ over land (the diagram over ocean would look different since maxima appear during local night). t_{on} is defined

365   as the time when Prec starts to increase and t_{on}^B is defined as the time when IWC^B starts to increase. Our two main

hypotheses are to assume that: i) IWC^B starts to increase later than Prec (a delay δt^B is assumed) because convective

systems precipitate before reaching UT and TL, as follow:

$$t_{on}^B = t_{on} + \delta t^B \tag{2}$$

and ii) the $IWC^B(t)$ is proportional to the $Prec(t)$ during the convective growing phase (see the period of proportionality in

370   Fig. 10). This hypothesis considers deep convection represented by Prec as the main process bringing ice into the UT and the

TL during the growing phase of the convection. Based on these two hypotheses and knowing $Prec_x$ and IWC_x^B at t_x and

t_{on}^B, we estimate $IWC^B\left(t_{on}^B\right)$ as follows:

$$IWC^B\left(t_{on}^B\right) = \frac{Prec\left(t_{on}^B\right)}{Prec_x} \times IWC_x^B \tag{3}$$

where x= *Day* or *N*. We use $t_x = t_{Day}$ for land since only the Day measurement occurs during the growing phase over land,

375   and $t_x = t_{Night}$ over sea since only the Night measurement occurs during the growing phase over ocean. Knowing $IWC^B\left(t_{on}^B\right)$

and t_{on}^B, the time evolution $IWC^B(t)$ during the growing phase is then:

$$IWC^B(t) = \left| \begin{array}{ll} \dfrac{Prec(t)}{Prec\left(t_{on}^B\right)} \times IWC^B\left(t_{on}^B\right) & \text{if } Prec(t) > Prec\left(t_{on}^B\right) \qquad (4) \\ \\ IWC^B\left(t_{on}^B\right) & \text{else.} \qquad\qquad\qquad\qquad\quad (5) \end{array} \right.$$

380   Our method can then estimate the magnitude of the diurnal variation in the UT and the TL $\left(\Delta IWC^B\right)$ over different regions

of the tropics:

$$\Delta IWC^B = IWC^B(t_{end}) - IWC^B(t_{on}^B) = IWC_{max}^B - IWC_{min}^B \tag{6}$$

with t_{end} being the time of the diurnal maximum of Prec. t_{end} can be considered as the time of the end for ice injection or the time from which the downdraft processes are more important than the updraft processes. Thus, we define δt_{end}^{UT} as the delay between t_{end} and t_{end}^{UT}. Following the hypothesis ii that considers that deep convection is the main process bringing ice into the UT and the TL, calculated ΔIWC^B represents the amount of ice injected by deep convection in these two layers. Thus, the duration of the injection of ice during the growing phase, Δt^B is then:

$$\Delta t^B = t_{end} - t_{on}^B \tag{7}$$

In order to validate this method, we compare the estimation of the amount of ice injected $\left(\Delta IWC^B\right)$ into the UT and the TL with the amount of ice measured in the troposphere and in the TL by the SMILES instrument on board the ISS during the short convective period of December 2009 to February 2010.

4.2 Evaluation of the method with SMILES measurements

The SMILES instrument measured IWC between 120 and 80 hPa and the overall measurement of tropospheric ice, the partial Ice Water Path (pIWP) integrated between 1000 and 180 hPa, from October 2009 to April 2010. This period is an El Nino Southern Oscillation (ENSO) period, increasing the convective activity over South Africa and the Western Pacific Ocean and decreasing the convective activity over the MariCont region and South America. The diurnal cycle of IWC and pIWP calculated from SMILES has shown the well separated signal over tropical land and ocean (Millán et al., 2013; Jiang et al., 2014). The anomalies of the diurnal cycle of IWC measured by SMILES near the TL, the diurnal cycle of pIWP in the troposphere and the diurnal cycle of Prec measured during the convective period of December 2009 to February 2010 are presented in Figure 11a over the three land study zones and in Figure 11b over the three ocean study zones, both with a running average of 6 h. t_{on}, t_{on}^{UT} and t_{on}^{TL} are the times of the minimum of Prec $(Prec_{min})$, pIWP $(pIWP_{min})$, and IWC $(pIWP_{min})$, respectively.

Over land, during the growing phase, pIWP is proportional to Prec (Fig. 11a). Assuming that IWC^{146} evolves like pIWC, this implies that $t_{on}^{UT} \approx t_{on}\left(\delta t_{on}^{UT} = 0\right)$ at ~ 08:00-09:00 LT, and $t_{end}^{UT} \approx t_{end} + \delta t_{end}^{UT}$ at ~ 16:00-17:00 LT, with $\delta t_{on}^{UT} \le 1$ h and $\delta t_{end}^{UT} \le 1$ h. Then, pIWP decreasing phase follows the same time evolution as Prec reaching minima (Prec$_{min}$ and $pIWP_{min}$) around 07:00-09:00 LT. Thus, ice in the troposphere follows the same diurnal cycle as the Prec within a time resolution of one hour.

In the TL, IWC is still proportional to Prec but IWC starts to increase later than $\left(\delta t_{on}^{TL} \sim 1\,h\right)$ the pIWP in the UT (Fig. 11a). After t_{end}, IWC decreases more rapidly than Prec and varies between +2 and -7 % compared to the mean between 23:00 and 09:00 LT. Thus, as soon as the deep convection reaches one of these two levels, ice is brought by the updraft during the growing and mature stage of the convective activity. Then, ice decreases with the downdraft of the convective dissipating

stage. However, the very deep convective activity reaching the TL starts later than the deep convection reaching the UT ($\delta t \approx$ 1 h) and decreases quickly before reaching a background IWC minimum between 23:00 LT and 09:00 LT.

Over ocean during the growing phase (Fig. 11b), pIWP also increases proportionally to Prec.Assuming that IWC[146] evolves

415 like pIWC, this implies that $t_{on}^{UT} \approx t_{on} + \delta t_{on}^{UT}$ $\left(\delta t_{on}^{UT} \geq 1 h \right)$ at ~21:00-22:00 LT, and $t_{end}^{UT} \approx t_{end} + \delta t_{end}^{UT}$ at ~ 04:00-05:00 LT with $\delta t_{end}^{UT} > 1$ h. Thus, as $\delta t_{on}^{UT} \approx \delta t_{end}^{UT}$, the diurnal cycle of pIWP over ocean is synchronized with the diurnal cycle of Prec but delayed. In the TL and during the growing phase, IWC starts to increase later than pIWP (where $\delta t_{on}^{TL} \approx 15$ h, Fig. 11b). This result is consistent with the diurnal cycle of OPF presented in Figure 9, where OPF starts to increase with a delay $\delta t_{on}^{TL} \approx 9$ h with respect to the increase of Prec.According to Liu and Zipser (2005), only less than 5% of OPF reach the TL, so other

420 processes in addition to deep convection govern the ice diurnal cycle in the TL over ocean impacting on the delay between the onset of ice injection t_{on}^{TL} and the onset of the convection t_{on}. After t_{on}^{TL}, IWC takes around 13 h to reach a maximum at t_{end}^{TL} ~ 19:00-20:00 LT.

Table 2 presents the magnitude of diurnal variation of ice, that is to say, the amount of ice injected into the UT and the TL estimated using the model presented in section 4.2 from the MLS and TRMM measurements (ΔIWC^B) and the magnitude of

425 diurnal variation of ice measured by SMILES ($\Delta pIWP$ and ΔIWC_{SMILES}) over the six study zones and during DJF 2009-2010. ΔIWC^{UT} and ΔIWC^{TL} are close to $\Delta pIWP_{SMILES}$ and ΔIWC_{SMILES}, respectively (with differences between 0.02 to 0.28 mg m^{-3}). Thus, during the ENSO period of DJF 2009-2010, the amount of ice injected in the UT $\left(\Delta IWC^{UT} \right)$ is about 2.06-2.34 mg m^{-3} over land and 1.20-1.22 mg m^{-3} over ocean and in the TL $\left(\Delta IWC^{TL} \right)$ is about 0.26-0.31 mg m^{-3} over land and 0.13-0.22 mg m^{-3} over ocean. NOAA Interpolated Outgoing Longwave Radiation (OLR) during DJF 2009-2010 is lower over land (mean

430 OLR between 195 and 215 W m^{-2} (not shown)) than over ocean (between 235 and 270 W m^{-2}) which is consistent with the more intense land convective activity compared to that of oceans.

In summary, our method based on the correlation between Prec from TRMM and IWC from MLS during the growing stage of the convection (presented in section 4.1) allows to estimate the amount of ice injected into the UT and the TL (ΔIWC^B) and has been validated with the SMILES measurements over land and ocean. These results confirm that the diurnal cycle of

435 Prec can be used as proxy of deep convection reaching the UT and the TL during the growing stage of the deep convection. The analyses of SMILES data also suggest a good correlation of IWC^{UT} and Prec during the dissipating stage of the convection in the UT over land.

4.3 Amount of ice injected in the austral convective UT

440 Using the method presented in the previous section, 13 years of MLS and TRMM observations are analysed. Table 3 presents the time of the beginning of the IWC injection in the UT $\left(t_{on}^{UT} \right)$, the duration of the IWC injection $\left(\Delta t^{UT} = t_{end} - t_{on}^{UT} \right)$,

the minimum value of IWC before the beginning of the IWC injection $\left(IWC_{min}^{UT}\right)$ and the amount of ice injected in the UT (equivalent to the amplitude of the IWC diurnal cycle, $\Delta IWC^{UT} = IWC_{max}^{UT} - IWC_{min}^{UT}$).

Over land, t_{on}^{UT} is found during the morning at 08:00-09:00 LT whatever the land zone. However, Δt^{UT} is longer over MariCont-L than SouthAm and SouthAfr (Δt^{UT} = 8, 7 and 7 h, respectively). Furthermore, IWC_{min}^{UT} is lower over the MariCont-L than over SouthAm and SouthAfr (IWC_{min}^{UT} = 1.04, 1.65 and 1.33 mg m^{-3}, respectively), but ΔIWC^{UT} is greater over the MariCont-L than over SouthAm and SouthAfr (ΔIWC^{UT} = 3.34, 1.99 and 2.86 mg m^{-3}, respectively).

Over ocean, t_{on}^{UT} is found during the evening at 17:00-18:00 LT. Δt^{UT} is much longer over MariCont-O than over IndOc and PacOc (Δt^{UT}= 11, 9, 9 h, respectively). However IWC_{min}^{UT} ,is greater over MariCont-O than over IndOc and PacOc (IWC_{min}^{UT} = 1.62, 1.01 and 1.46 mg m^{-3} respectively) and ΔIWC^{UT} over MariCont-O is also greater than ΔIWC^{UT} over PacOc and IO $\left(\Delta IWC^{UT}\right.$ = 0.91, 0.46 and 0.43 mg m^{-3}, respectively).

Thus, the convective growing stage is quicker over land (7 h) than over ocean (10 h). These results are consistent with previous study from Takahashi and Luo (2014) showing that the time life of the mature stage of the deep convection is between 6 and 12 h after the onset of the deep convection considering North and South hemispheres over the tropics. Furthermore, while the estimated means of IWC_{min}^{UT} over land and ocean are very close (1.34 and 1.36 mg m^{-3}, respectively), the means of the land and ocean ΔIWC^{UT} show great differences (2.73 and 0.60 mg m^{-3}, respectively). Thus, the ice minima are of similar amplitudes over land and ocean in the UT but the amount of ice injected in the UT is about 4 times greater over land than over ocean. These results also show that the MariCont region is a region with greater amount of ice injection in the UT compared to other tropical deep convective areas.

4.4 Amount of ice injected in the austral convective TL

From the method presented previously and the results from the SMILES instruments (Fig. 11), Table 4 presents t_{on}^{TL}, Δt^{TL}, IWC_{min}^{TL} and ΔIWC^{TL} with respect to time for ice to be injected into the TL after the onset of deep convection, δt^{TL} over the different study zones. We propose to use δt^{TL} = 0 to 3 h in order to keep δt^{TL} always shorter than t_{on}-t_x, where x is selected during the growing phase (x=D over land and x=N over ocean) in order to perform a sensitivity study of our results.

Over land, for all t_{on}^{TL}, the period of injection $\left(\Delta t^{TL}\right)$ is longer over MariCont-L than over SouthAm and SouthAfr (Δt^{TL} = 8, 7 and 7 h, respectively). Depending on the δt^{TL} (between 0 and 3 h), Δt^{TL} can be between 7-8 and 4-5 h. ΔIWC^{TL} is greater over MariCont-L than over SouthAm and SouthAfr for all the δt^{TL} (ΔIWC^{TL} ~ 0.56-0.42, 0.26-0.13 and 0.40-0.24 mg m^{-3}, respectively). As observed in the short time period study with SMILES, the injection of ice over MariCont-L is the most intense over tropics. Furthermore, the smaller δt^{TL}, the longer Δt^{TL}, the greater ΔIWC^{TL} .

Over ocean, as observed with the SMILES measurements, t_{on}^{TL} cannot be estimated with our method. However, our method is able to estimate Δt^{TL}, IWC_{min}^{TL} and ΔIWC^{TL} as a function of δt^{TL} (as demonstrated in section 4.1). Over MariCont-O, ice injection in the TL is longer than over IndOc and PacOc (Δt^{TL} = 8-11, 6-9 and 6-9 h, respectively). The amount of ice injected over MariCont-O is greater than over IndOc and PacOc (ΔIWC^{TL} = 0.16-0.19, 0.09-0.10, 0.08-0.09 mg m^{-3},

475   respectively). Furthermore, the ice background in the TL is also greater over MariCont-O than over IndOc and PacOc (IWC_{min}^{TL} ~ 0.34-0.37, 0.24-0.26, 0.29-0.30 mg m^{-3}, respectively). Thus, while the diurnal cycle of Prec over MariCont-O is the weakest, the diurnal cycle of ice over MariCont-O would have the highest values.

As expected from the SMILES measurements, the MariCont region presents the largest ice injection in the TL. While the IWC background over MariCont-O is the largest, the injection of IWC over MariCont-L is the most important.

480

5. Discussion on the processes driving the decreasing phase of the IWC diurnal cycle

The previous section has shown that the growing phase of the diurnal cycle of deep convection in the tropics impacts on the growing phase of diurnal cycle of ice in the UT and the TL. In this section, the convective processes impacting the

485   decreasing phase of the ice diurnal cycle in the UT and the TL are discussed. The decreasing phase of the diurnal cycle of ice in the UT and the TL represents the diurnal loss of ice. This loss can be caused by several processes including sedimentation, downdraft convective processes during the dissipating stage, sublimation into water vapour or horizontal advection and mixing. Quantifying the processes impacting the diurnal cycle of ice can help to quantify the amount of water staying into the UT and TL, the part falling down to the surface and the part advected up to the LS at the temporal diurnal scale.

490   In this section, the comparison between the value of IWC measured by MLS during the decreasing phase (IWC_x) at (x = Day or Night) and IWC estimated at the same t_x ($IWC(t_x)$) is discussed. If $IWC_x \sim IWC(t_x)$, our model based on Prec evolution is a good predictive tools to consider that convective processes (as represented by Prec) control the decreasing phase of the ice diurnal cycle. Otherwise, non-convective processes has also need to be investigated to explain the ice diurnal cycle. Table 5 presents the difference d ($d = IWC(t_x) - IWC_x$) in the UT and the TL.

495   Over land in the UT, d is positive and less than 23 % over SouthAm and SouthAfr and close to zero over the MariCont-L. The fact that the amount of Prec over SouthAm and SouthAfr is greater than required to explain IWC suggests that a significant fraction of the convection is shallow and does not reach the UT. In contrast, over the MariCont-L, the diurnal cycle of Prec is very similar to the diurnal cycle of IWC suggesting that the convective activity over this region brings a large amount of ice all over the 24 hours. In the TL, d is found between -14 and -20 % implying that the ice decreases more

500   slowly than Prec.

Over ocean in the UT, d is negative down to -26 % showing that the ice stay longer in the UT compared to the Prec decreasing phase. In the TL, d varies between +9 and -7 showing low differences d at this level.

In summary, the method presented in the present paper allows to estimate the diurnal cycle of ice in the UT and the TL to

within 26 % over the 6 tropical zones and to within 14 % over the MariCont-L region.

6. Conclusion and perspectives

To quantify the amount of ice injected in tropical upper troposphere (UT) and the tropopause layer (TL) and the processes linked to the ice diurnal variation is important to better understand the amount of total water in these layers and the amount
510 of water entering into the LS. The information given by MLS on the diurnal cycle of ice water content (IWC) in the UT and the TL and the method comparing the two per day measurements (Liu and zipser, 2005 and Carminati et al., 2014) are too limited to estimate the ice variability in these layers. Thus, the present study starts to assume that the diurnal cycle in ice is related to the diurnal cycle in precipitation (for which there are TRMM data with much better time resolution) in austral convective tropics. The high relationship between precipitation (Prec) measured by TRMM and IWC measured by MLS in
515 the UT and the TL is shown in the study. As MLS measures IWC only twice a day, at 01:30 (Night) and 13:30 LT (Day), we have proposed a simple model based on the diurnal cycle of Prec to estimate the diurnal cycle of IWC in the UT and in the TL. The method is validated using the short period of DJF 2009-2010 of ice measurement from the SMILES instrument in the troposphere and the TL.

Because of the strong space correlation between Prec and IWC, we show that Prec can be used as a proxy of the deep
520 convection reaching the UT and the TL during the growing stage of the convection in order to bring ice in the UT and the TL. The method proposed in the study allows to estimate 1) the diurnal cycle of ice into the UT and the TL and 2) the difference between the maximum and the minimum in the diurnal cycle of ice in these layers, namely the amount of ice injected by deep convection. Our method suggests that deep convection is the most important process in austral convective tropics driving the diurnal increase of ice in these layers. Other processes may play a minor role such as the decrease of the
525 temperature in the TTL, increasing the saturation ratio and allowing the crystal nucleation and growth, or the bring of ice in the UT and TL by horizontal advection.

The amount of ice injected in the UT (2.73 mg m^{-3} over land and 0.60 mg m^{-3} over ocean) is found to be much higher than the amount of ice injected in the TL (0.26-0.41 mg m^{-3} over land and 0.11-0.13 mg m^{-3} over ocean). Furthermore, the study highlights the importance to separate the land of the Maritime Continent (MariCont-L) to the ocean of the Maritime
530 Continent (MariCont-O) to better understand the ice diurnal cycle in the UT and the TL over the complex and strong convective region of the Maritime Continent. It has been shown that the injection of ice over the MariCont-L into the UT and the TL (ΔIWC^{UT} = 3.34 mg m^{-3}, ΔIWC^{TL} = 0.56-0.42 mg m^{-3}) is the greatest in the tropics. This injection of ice would have a strong importance on the amount of ice entering into the LS and feeding what has been called the 'stratospheric fountain' (Newell and Gould-Stewart, 1981) observed over the MarCont region.
535 The decreasing phase of the ice diurnal cycle is also evaluated with Prec and discussed. While, it is difficult to quantify the impact of other processes than convective processes on the diurnal cycle of ice in the UT and the TL, we are able to assess that the deep convection impacts on the depletion of ice during the decreasing phase of the ice diurnal cycle (from Table 5:

97 % in the UT over the MariCont and ~80 % in averaged UT and TL over other regions). Thus, Prec is also considered to be a good proxy of the decreasing phase of the convection, especially over the MariCont-L region in the UT (to within 3 %, according to Table 5), and convective processes are the main processes impacting the decreasing phase of the diurnal cycle of ice. Furthermore, our study has shown that the estimated diurnal variation of ice is the largest in the regions (identified from TRMM) where the diurnal variation in temperature is also the largest although horizontal transport may play a role, but it cannot be quantified using our methodology.

In summary, while the importance of deep convective processes and large-scale three-dimensional circulation processes on the ice and water injection up to the UT, TL and LS are still debated, this study shows that the ice diurnal cycle in the UT and the TL is mainly governed by vertical processes linked to the convective activity that are much stronger than other processes such as e.g. horizontal mixing, sublimation, sedimentation, ...

Although it is beyond the scope of the present paper, some potentially new results might be achievable using our method as e.g. the part of ice sublimating during deep convection, the impact of intra-seasonal variability such as ENSO and the Madden Julian Oscillation (MJO) on the ice diurnal cycle. In fact, ENSO and MJO have a strong influence on the tropical deep convection and injection of moisture into the TTL (Gettelman et al., 2002; Wong and Dessler, 2007) and are associated to the cold anomalies near the TTL, especially over the Maritime Continent region (Zhang et al., 2013). We are expecting a strong impact on the diurnal ice injection timing and duration in the TL. The processes impacting the ice injection into the UT and the TL over the Maritime Continent regions at local scale will be studied in a forthcoming paper.

Author contribution

IAD analysed the data, formulated the model used to combine MLS and TRMM data and took primary responsibility for writing the paper. PR and PH contributed to the design of the study, the interpretation of the results and the writing of the paper. FC provided advice on MLS data processing, TC contributed to discussion of the overall results and both FC and TC provided comments on the paper.

Acknowledgement

Our study takes place within the Turbulence Effects on Active Species in Atmosphere (TEASAO – http://www.legos.obs-mip.fr/projets/axes-transverses-processus/teasao) project. We thank the National Center for Scientific Research (CNRS) and the Excellence Initiative (Idex) of Toulouse, France (TEASAO project, Peter Haynes Chair of Attractivy) to fund this study. We would like to thank the teams that have provided the MLS data (https://disc.gsfc.nasa.gov/datasets/ML2IWC_V004), the TRMM data (https://pmm.nasa.gov/data-access/downloads/trmm) and the SMILES data (https://mls.jpl.nasa.gov/data/smiles).

References

Alcala, Dessler, A. E.: Observations of deep convection in the tropics using the Tropical Rainfall Measuring Mission (TRMM) precipitation radar, J. of Geo. Res., vol. 107, NO. D24, 4792, doi:10.1029/2002JD002457, 2002.

Allison, T., Fuelberg, H., Heath, N.: Simulations of Vertical Water Vapor Transport for TC Ingrid (2013). J. of Geophys. Res.: Atmospheres, 123(15), 8255-5282, doi: 10.1029/2018JD028334, 2018.

Avery, M. A., Davis, S. M., Rosenlof, K. H., Ye, H. and Dessler, A. E.: Large anomalies in lower stratospheric water vapour and ice during the 2015-2016 El Nino, Nat. Geosci., 10(6), 405–409, doi:10.1038/ngeo2961, 2017.

Beucher, F.: Manuel de météorologie tropicale: des alizés au cyclone tropical, Météo-France, Paris, France, 2010.

Birner, T. and Charlesworth, E. J.: On the relative importance of radiative and dynamical heating for tropical tropopause temperatures, J. Geophys. Res. Atmospheres, 122(13), 6782-6787, doi:10.1002/2016JD026445, 2017.

Carminati, F., Ricaud, P., Pommereau, J.-P., Rivière, E., Khaykin, S., Attié, J.-L., and Warner, J.: Impact of tropical land convection on the water vapour budget in the tropical tropopause layer, Atmos. Chem. Phys., 14, 6195-6211, doi:10.5194/acp-14-6195-2014, 2014.

Corti, T., Luo, B. P., Fu, Q., Vömel, H. & Peter, T.: The impact of cirrus clouds on tropical troposphere-to-stratosphere transport. Atmos. Chem. and Phys. 6, 2539–2547, doi:10.5194/acp-6-2539-2006, 2006.

Corti T, Luo BP, Reus M de, Brunner D, Cairo F, Mahoney MJ: Unprecedented evidence for deep convection hydrating the tropical stratosphere. Geophys. Res. Letters., 35(10), doi:10.1029/2018GL033641, 2008.

Dauhut, T., Chaboureau, J.-P., Escobar, J., Mascart, P.: Large-eddy simulations of Hector the convector making the stratosphere wetter. Atmos. Sci. Letters 16, 135–140., doi:10.1002/asl2.534, 2015.

Fueglistaler, S., Dessler, A. E., Dunkerton, T. J., Folkins, I., Fu, Q. and Mote, P. W.: Tropical tropopause layer, Rev. Geophys., 47(1), RG1004, doi:10.1029/2008RG000267, 2009.

Gettelman, A. and Forster, P. M. de F.: A Climatology of the Tropical Tropopause Layer, J. Meteorol. Soc. Jpn. Ser II, 80(4B), 911–924, doi:10.2151/jmsj.80.911, 2002.

Hartmann, D. L., Holton, J. R., Fu, Q.: The heat balance of the tropical tropopause, cirrus, and stratospheric dehydration. Geo. Res. Letters 28, 1969–1972, 2001.

Holton, J. R. and Gettelman, A.: Horizontal transport and the dehydration of the stratosphere, Geophys Res Lett, 28(14), 2799–2802, doi: 10.1029/2001GL013148, 2001.

Jensen, E. J., Toon, O. B., Pfisher, L., Selkirk, H. B.: Dehydration of the upper troposphere and lower stratosphere by subvisible cirrus clouds near the tropical tropopause, Geophys Res Lett, doi: 10.1029/96GL00722, 1996.

Jensen, E. J., Smith, J. B., Pfister, L., Pittman, J. V., Weinstock, E. M., Sayres, D. S., Wilson, J. C.: Ice supersaturations exceeding 100% at the cold tropical tropopause: implications for cirrus formation and dehydration. Atmospheric Chemistry and Physics, 5(3), 851–862, doi: 10.5194/acp-5-851-2005, 2005.

Jensen, E. J.: Physical processes controlling ice concentrations in synoptically forced, midlatitude cirrus. J. of Geophys. Res.:

Atmospheres, 118(11), 5348-5360, doi: 10.1002/jgrd.50421, 2013.

Jiang, J. H., Su, H., Zhai, C., Janice Shen, T., Wu, T., Zhang, J., et al.: Evaluating the Diurnal Cycle of Upper-Tropospheric Ice Clouds in Climate Models Using SMILES Observations. J. Atmos. Sci. 72, 1022–1044., doi:10.1175/JAS-D-14-0124.1, 2014.

610 Khaykin, S., Pommereau, J.-P., Korshunov, L., Yushkov, V., Nielsen, J., Larsen, N., Christensen, T., Garnier, A., Lukyanov, A., and Williams, E.: Hydration of the lower stratosphere by ice crystal geysers over land convective systems, Atmos. Chem. Phys., 9, 2275-2287, doi: 10.5197/acp-9-2275-200, 2009.

Khaykin, S. Mk., J.-P. Pommereau and A. Hauchecorne: Impact of land convection on temperature diurnal variation in the tropical lower stratosphere inferred from COSMIC GPS radio occultations, Atmos. Chem. Phys., 13, 6391-6402, doi: 615 10.5194/acp-13-6391-2013, 2013.

Khaykin, S. M., Pommereau, J.-P., Riviere, E. D., Held, G., Ploeger, F., Ghysels, M., Armarouche, N., Vernier, J.-P., Wienhold, F., G., Ionov, D.: Evidence of horizontal and vertical transport of water in the Southern Hemisphere tropical tropopause layer (TTL) from high-resolution balloon observations. Atmospheric Chemistry and Physics 16, 12273–12286, doi: 10.5194/acp-16-12273-2016, 2016.

620 Kim, J. and Son, S.-W. Tropical Cold-Point Tropopause: Climatology, Seasonal Cycle, and Intraseasonal Variability Derived from COSMIC GPS Radio Occultation Measurements. J. Climate, 25, 5343–5360, doi: 10.1175/JCLI-D-11-00554.1, 2012.

Liu, C. and Zipser, E. J.: Global distribution of convection penetrating the tropical tropopause, J. Geophys. Res. Atmospheres, 110(D23), D23104, doi:10.1029/2005JD006063, 2005.

Livesey, N. J., Read, W. G. and Wagner, P. A.: Version 4.2x Level 2 data quality and description document, 2017.

625 Mehta, S. K., Krishna Murthy, B. V., Narayana Rao, D., Venkat Ratnam, M., Parameswaran, K., Rajeev, K., Suresh Raju, C., Kusuma, G. Rao.: Identification of tropical convective tropopause and its association with cold point tropopause. J. Geophys. Res. 113, D00B04, doi: 10.1029/2007JD009625, 2008.

Millán, L., Read, W., Kasai, Y., Lambert, A., Livesey, N., Mendrok, J., Sagawa, H., Sano, T., Shiotani, M. and Wu, D. L.: SMILES ice cloud products, J. Geophys. Res. Atmospheres, 118(12), 6468–6477, doi:10.1002/jgrd.50322, 2013.

630 Nesbitt, S. W., Zipser, E. J., Cecil, D. J.: A Census of Precipitation Features in the Tropics Using TRMM: Radar, Ice Scattering, and Lightning Observations. J. Climate 13, 4087–4106, doi: 10.1175/1520-0442(2000)013<4087:ACOPFI>2.0.CO;2, 2000.

Newell, R. E. and Gould-Stewart, S.: A Stratospheric Fountain?, J. Atmospheric Sci., 38(12), 2789–2796, doi:10.1175/1520-0469(1981)038<2789:ASF>2.0.CO;2, 1981.

635 Pereira, L. G., Rutledge, S. A.: Diurnal Cycle of Shallow and Deep Convection for a Tropical Land and an Ocean Environment and Its Relationship to Synoptic Wind Regimes. Mon. Wea. Rev. 134, 2688–2701, doi: 10.1175/MWR3181.1, 2006.

Peter, T. et al.,: When Dry Air Is Too Humid. Science 314, 1399–1402., 2006.

Pommereau, J.-P.: Troposphere-to-stratosphere transport in the tropics. Comptes Rendus Geoscience 342, 331–338., doi:

640   10.1016/j.crte.2009.10.015, 2010.

Schoeberl, M. R., Jensen, E. J., Pfister, L., Ueyama, R., Avery, M., and Dessler, A. E.: Convective hydration of the upper troposphere and lower strato- sphere. Journal of Geophysical Research: Atmospheres, 123, 4583–4593., doi:10.1029/2018JD028286, 2018.

Solomon, S. et al. Contributions of Stratospheric Water Vapor to Decadal Changes in the Rate of Global Warming. Science

645   327, 1219–1223, doi: 10.1029/1999RG900008, 2010.

Suneeth, K. V., Das, S. S. and Das, S. K.: Diurnal variability of the global tropical tropopause: results inferred from COSMIC observations, Clim. Dyn., doi:10.1007/s00382-016-3512-x, 2017.

Takahashi, H., Luo, Z. J. Characterizing tropical overshooting deep convection from joint analysis of CloudSat and geostationary satellite observations. Journal of Geophysical Research: Atmospheres 119, 112–121, doi:

650   10.1002/2013JD020972, 2014.

TRMM. Available at: https://trmm.gsfc.nasa.gov/publications_dir/publications.html.

Ueyama, R., Jensen, E. J., Pfister, L. and Kim, J.-E.: Dynamical, convective, and microphysical control on wintertime distributions of water vapour and clouds in the tropical tropopause layer, J. Geophys. Res. Atmospheres, 120(19), 2015JD023318, doi:10.1002/2015JD023318, 2015.

655   Wright, J. S., Fu, R., Fueglistaler, S., Liu, Y. S., and Zhang, Y.: The influence of summertime convection over Southeast Asia on water vapor in the tropical stratosphere, J. Geophys. Res., 116, D12302, doi:10.1029/2010JD015416, 2011.

Wong, S., and Dessler, A., E.: Regulation of H2O an CO in tropical tropopause layer by the Madden-Julian oscillation, J. Geophys. Res., 112, D14305, doi:10.1029/2006JD007940, 2007.

Yang, G.-Y. and Slingo, J.: The diurnal cycle in the tropics, Mon. Weather Rev., 129(4), 784–801, doi: 10.1175/1520-

660   0493(2001)129<0784:TDCITT>2.0.CO;2, 2001.

Zhang, C.: Madden–Julian Oscillation: Bridging Weather and Climate. Bull. Amer. Meteor. Soc. 94, 1849–1870, doi:10.1175/BAMS-D-12-00026.1, 2013.

Zhou, C., Dessler, A. E., Zelinka, M. D., Yang, P., and Wang, T.: Cirrus feedback on interannual climate fluctuations, Geophys. Res. Lett., 41, 9166–9173, doi:10.1002/2014GL062095., 2014.

665

670
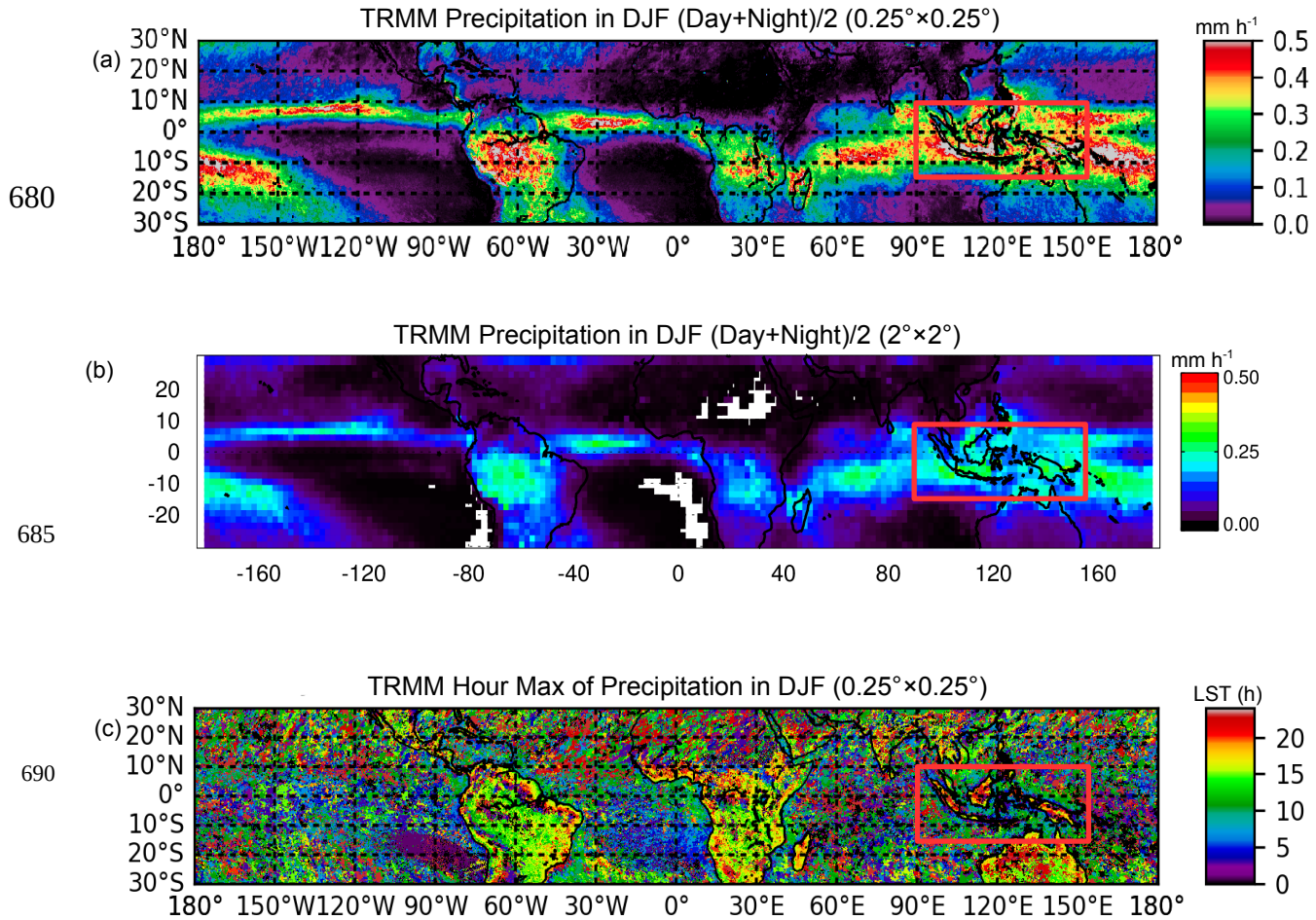
Figure 1: (From top to bottom): (a) (Day+Night)/2 of precipitation measured by TRMM at 0.25°×0.25° resolution (mm/h), (b) (Day+Night)/2 of precipitation at 2°×2° resolution (mm/h), and (c) hour of diurnal maximum of precipitation at 0.25°×0.25° resolution (h in Local Solar Time, LST) in DJF over the period 2004-2017. The red box surrounds the MariCont region.
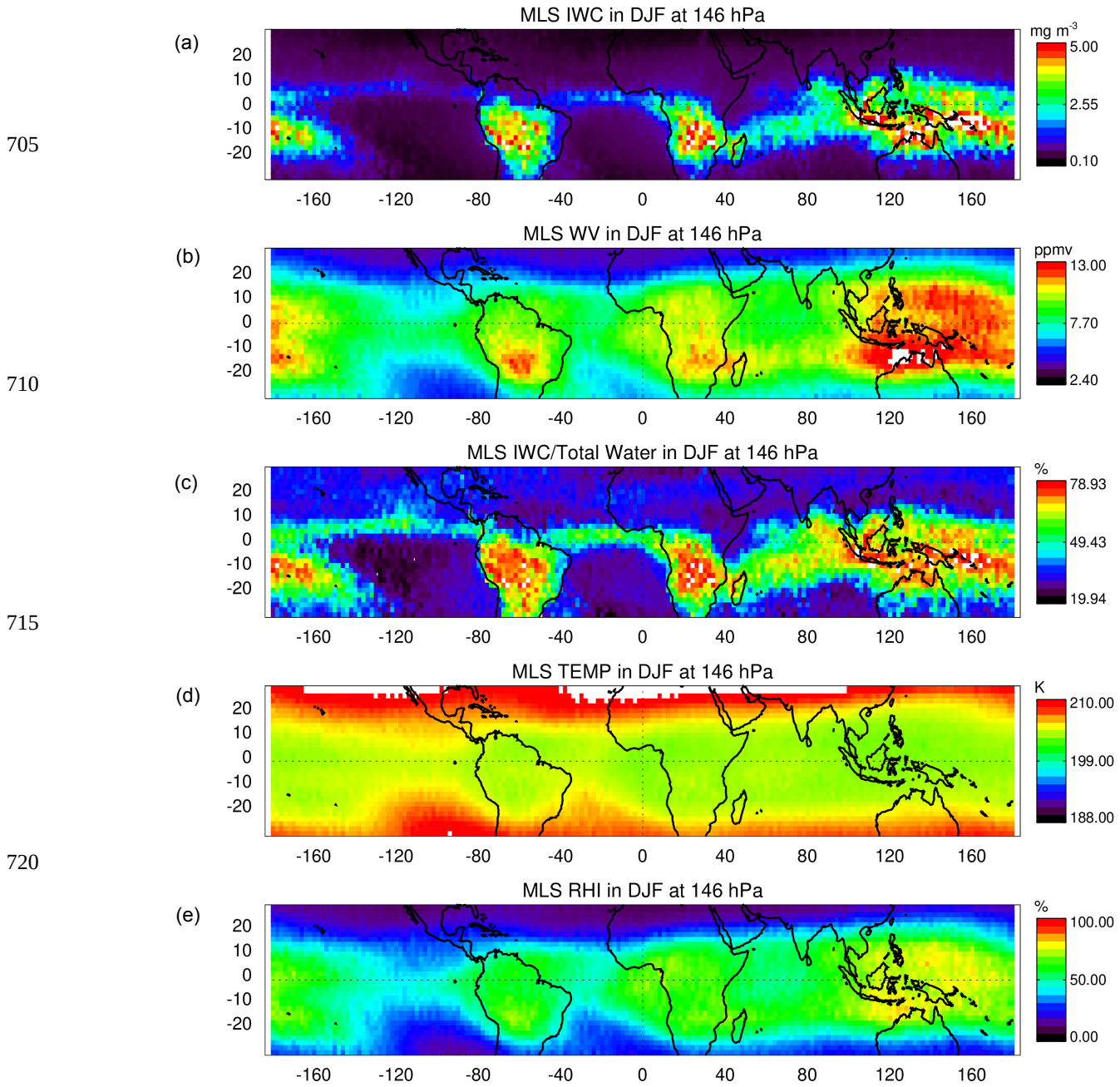
Figure 2: (From top to bottom): (a) daily average (Day+Night)/2 of Ice Water Content (IWC), (b) Water Vapour (WV), (c) IWC fraction (IWC/∑W), (d) Temperature and (e) Relative Humidity with respect to Ice (RHI) in the upper troposphere (146 hPa) measured by MLS over the tropics in DJF over the period 2004-2017.

730
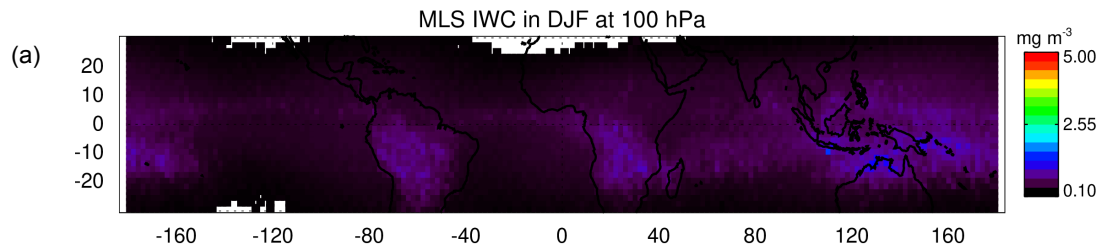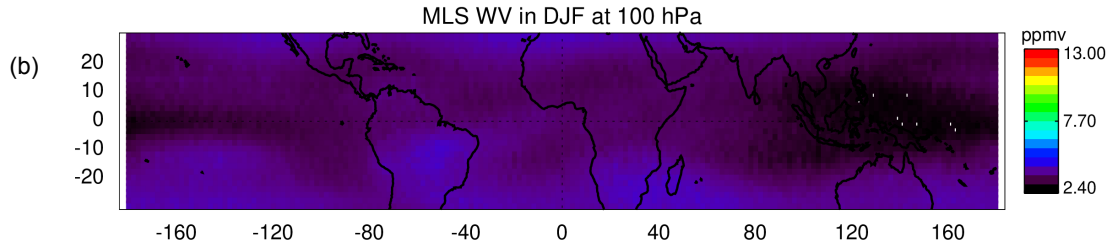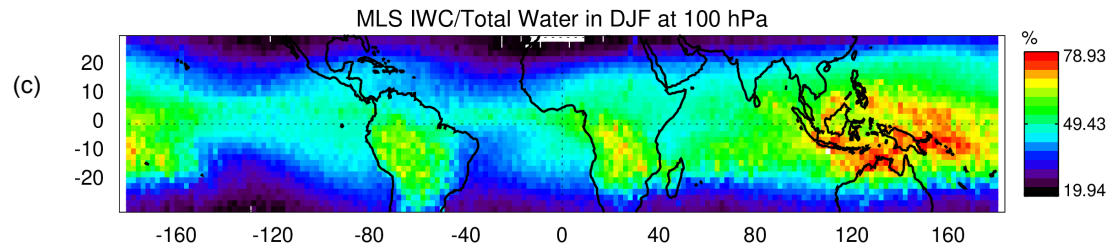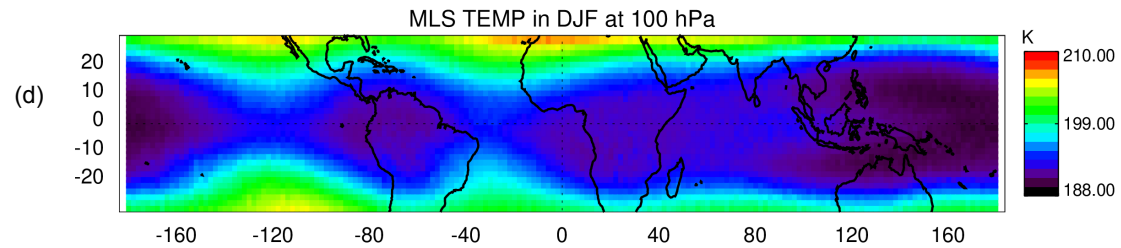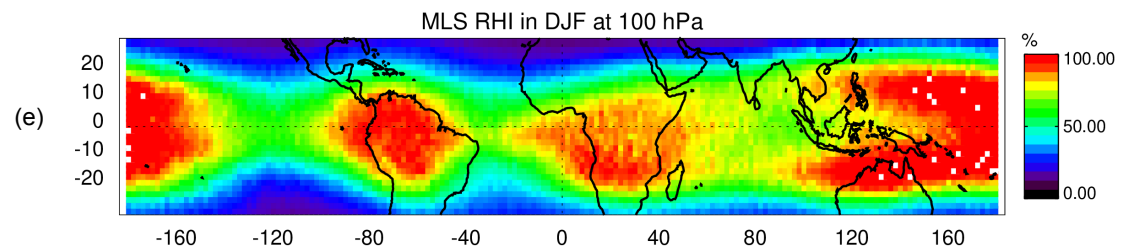
Figure 3: (From top to bottom): (a) daily average (Day+Night)/2 of Ice Water Content (IWC), (b) Water Vapour (WV), (c) IWC fraction (IWC/∑W), (d) Temperature and (e) Relative Humidity with respect to Ice (RHI) in the tropopause layer (100 hPa) measured by MLS over the tropics in DJF over the period 2004-2017.
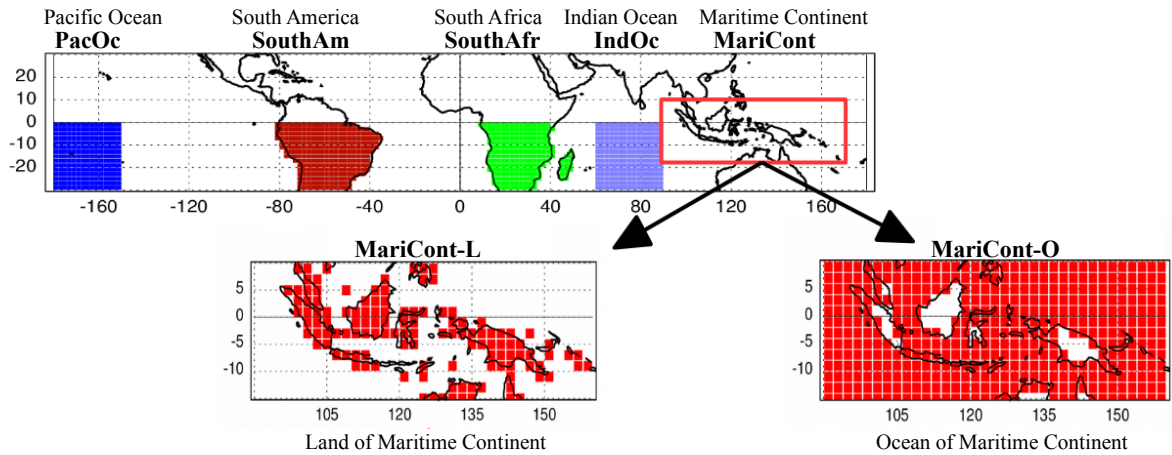
Figure 4: Representation of the study zones: PacOc, Pacific Ocean; SouthAm, South America; SouthAfr, South Africa; IndOc, Indian Ocean; MariCont-L, land of the Maritime Continent; MariCont-O, ocean of the Maritime Continent. Each zone is defined at a horizontal resolution of 2°×2°.
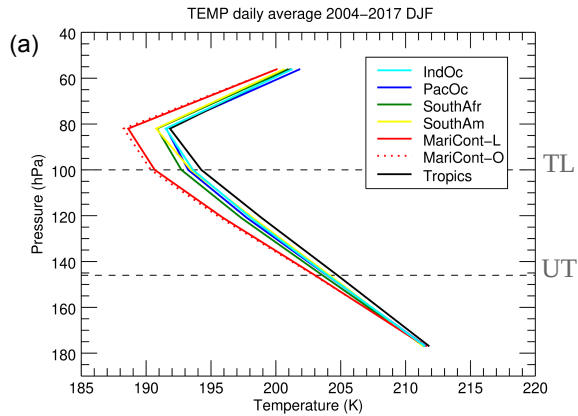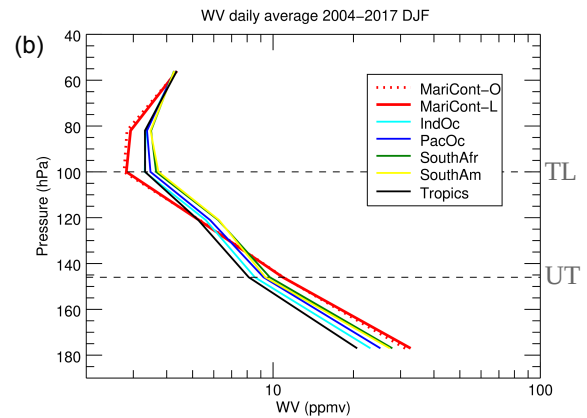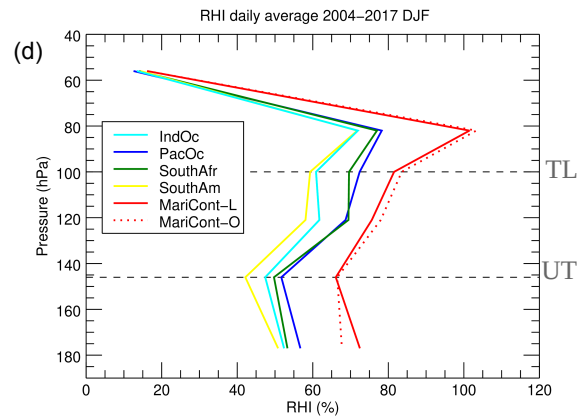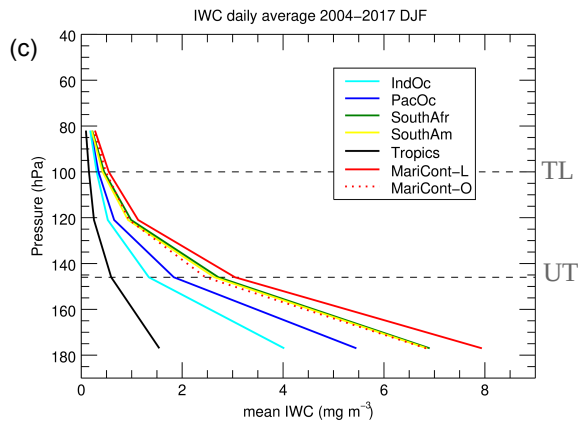
Figure 5: Vertical profiles of (a) temperature, (b) Water Vapour (WV), (c) Ice Water Content (IWC) and (d) Relative Humidity with respect to Ice (RHI) from MLS data averaged from 2004 to 2017 in DJF over the 6 study zones: IndOc (light blue), PacOc (dark blue), SouthAfr (green), SouthAm (yellow), Tropics (black), MariCont-L (red solid line) and MariCont-O (red dashed line).
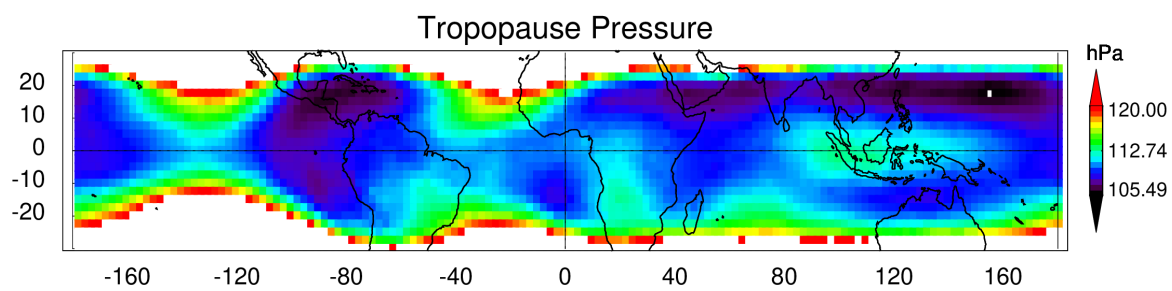
810 **Figure 6: Pressure of the tropopause (hPa) over the tropics during DJF from 2004 to 2017, defined from the NCEP datasets.**

815
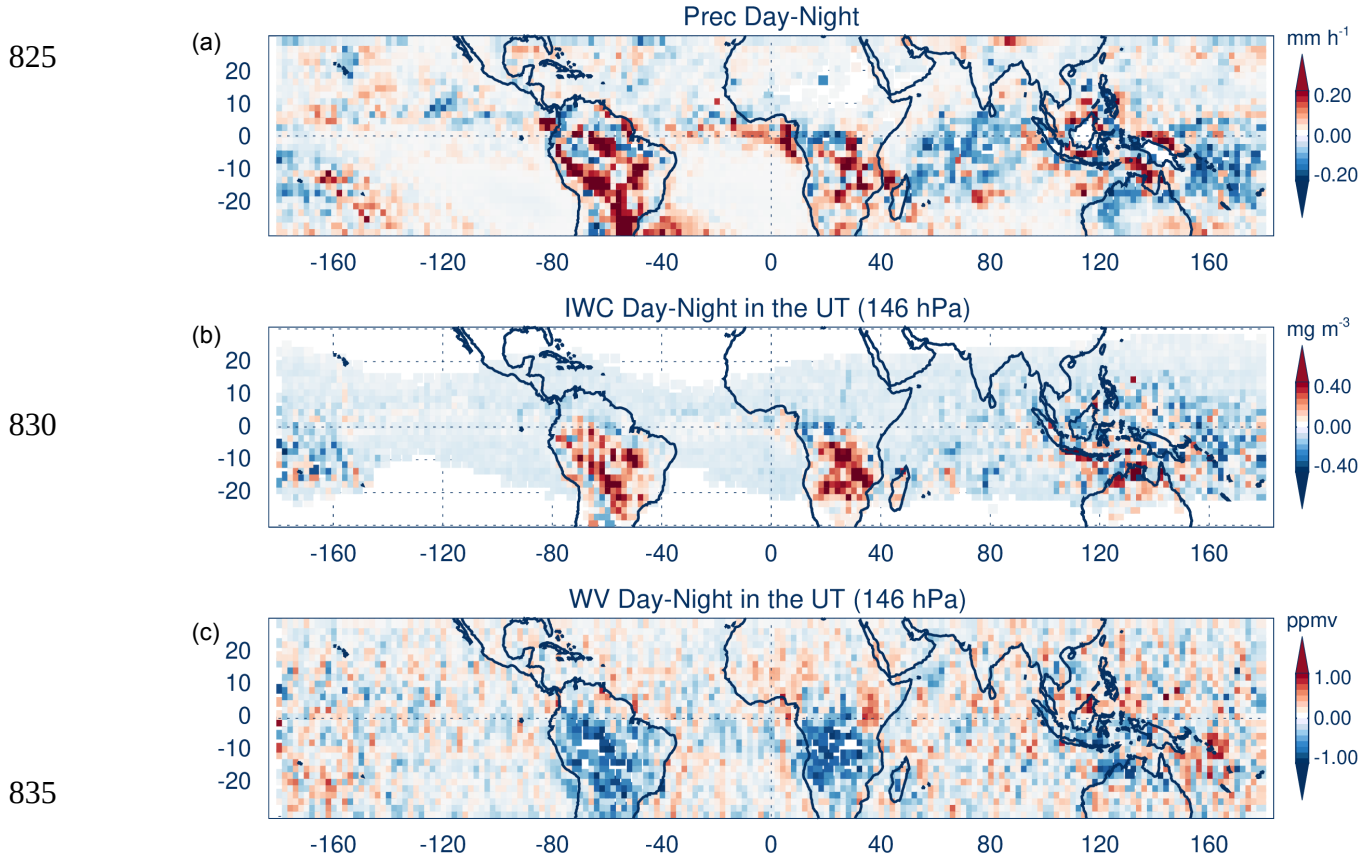
820

Figure 7: Day−Night of (a) precipitation (Prec) from TRMM, (b) Ice Water Content (IWC) from MLS at 146 hPa and (c) Water
 Vapour (WV) from MLS at 146 hPa over the tropics and the period 2004-2017 in DJF.
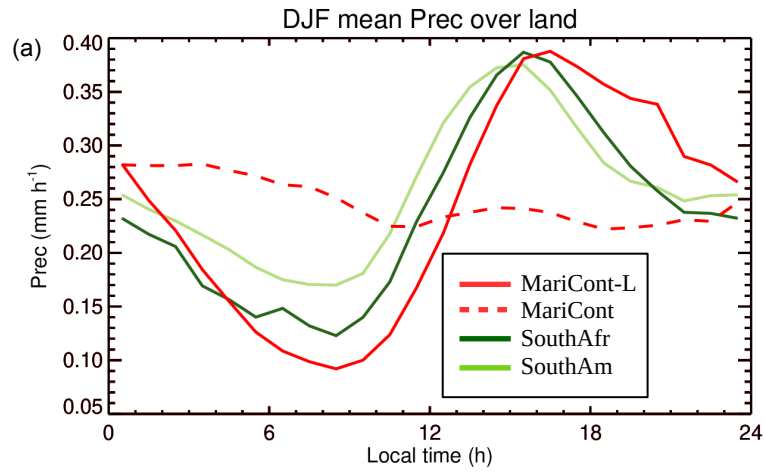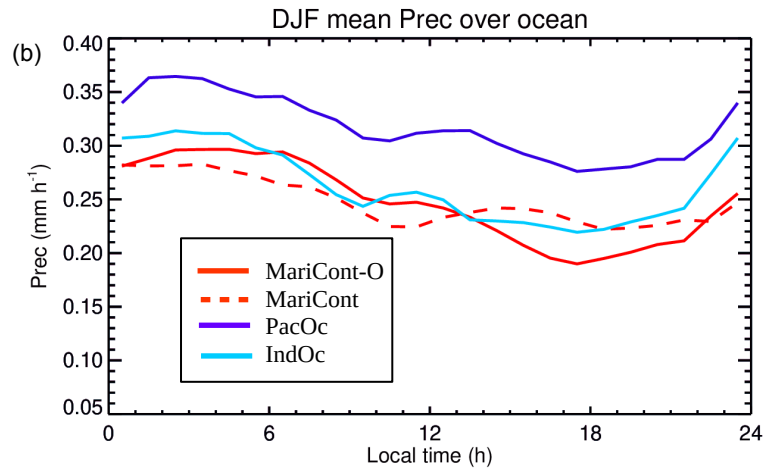
Figure 8: Diurnal cycle of precipitation (Prec) over (a) the land study zones and (b) the ocean study zones during the period DJF 2004-2017.
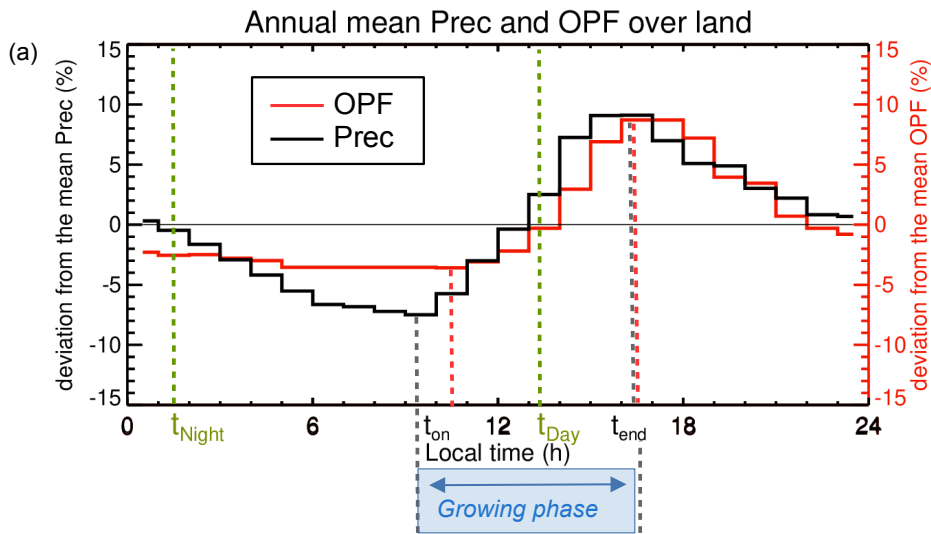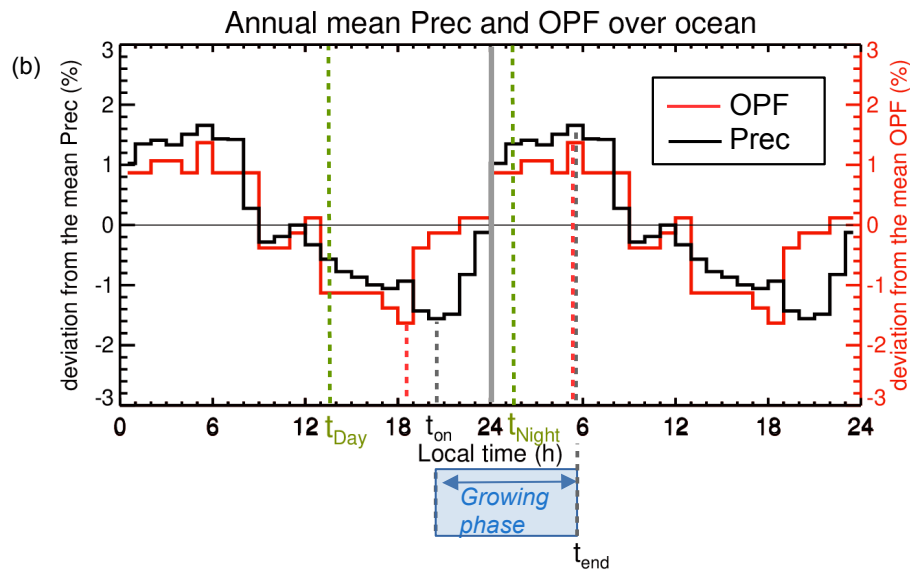
Figure 9: (Top) Deviation from the mean of the annual mean diurnal cycle of TRMM precipitation (Prec, in black solid line) over land, from 2004 to 2017 and diurnal cycle of overshooting precipitation features (OPFs) at the tropopause (red solid line) over land, from 1998 to 2000 and from 2001 to 2003 adapted from Liu and Zipser (2005) over the tropics (20°N-20°S). **(Bottom)** Same as top but over the ocean. Minimum and maximum of Prec and OPF are drawn with vertical dotted lines (in black and red, respectively). t_{on} is the time of the onset of the Prec, t_{end} is the time of the diurnal maximum of Prec, t_{Day} and t_{Night} are the times of the two MLS measurements at Day and Night, respectively.
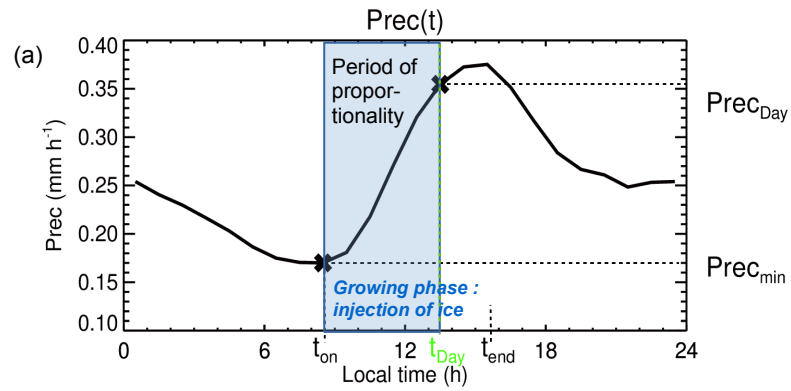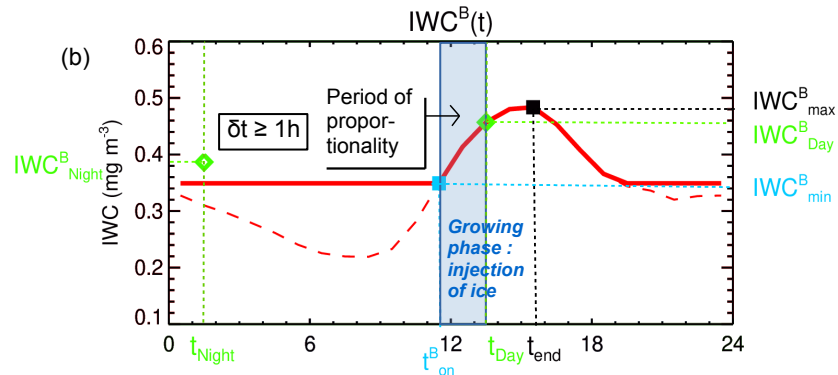
Figure 10: Methodology to estimate the diurnal cycle of ice water content (IWC) over land: (a) diurnal cycle of precipitation, with ✖ representing the minimum of precipitation $(Prec_{min})$ with its associated time (t_{on}) and Prec during the day $(Prec_{Day})$ at t_{Day} = 13:30 LT. (b) Diurnal cycle of $IWC^B(t)$ in red solid line, estimated from the diurnal cycle of Prec and from the two MLS measurements of ice (◇, IWC_x^B), with the timing of the onset of the ice injection at $t_{on}^B = t_{on} + \delta t^B$. ■ represents the IWC maximum (IWC_{max}^B) and ■, the IWC_{min}^B when $\delta t^B > 1h$. Note that when $t_{on} \approx t_{on}^B$, the diurnal cycle of IWC is the red dashed line.
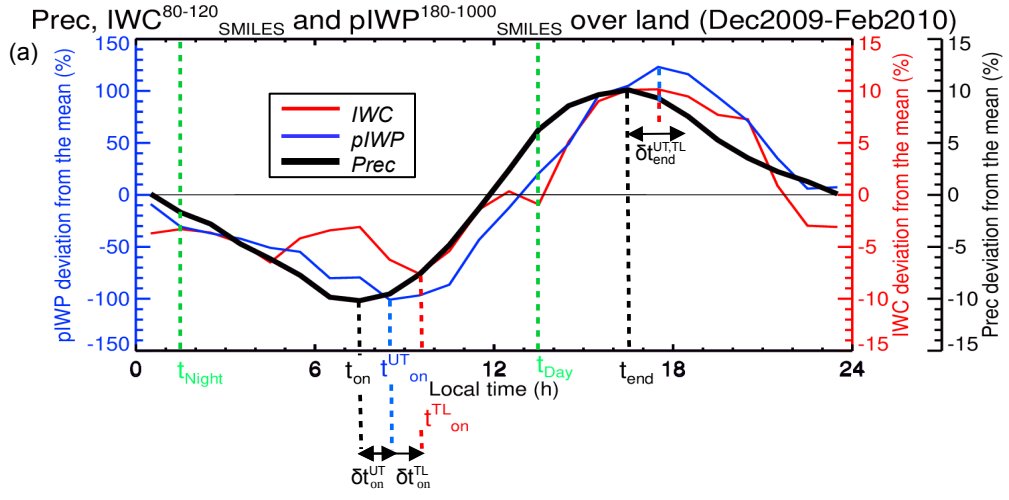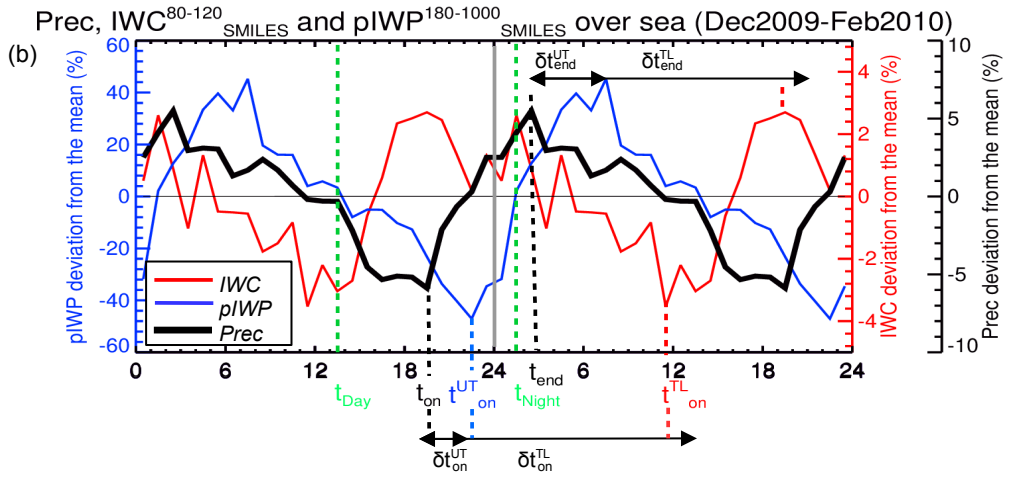
Figure 11: Deviation from the mean (%) of the diurnal cycle of partial Ice Water Path (pIWP, integrated between 1000 and 180 hPa), Ice Water Content (IWC, averaged between 80 and 120 hPa) measured by SMILES and precipitation (Prec) over (a) the tropical land (0°S-30°S) and (b) tropical ocean (0°N-30°S) from December 2009 to February 2010. t_{on}, t_{on}^{UT} and t_{on}^{TL} are the onset of the Prec, pIWP and IWC increase, respectively. t_{end} is the end of the Prec increase. δt_{on}^{UT} and δt_{on}^{TL} are the delay between t_{on} and t_{on}^{UT} and t_{on}^{TL}, respectively and δt_{end}^{UT} and δt_{end}^{UT} are the delay between t_{end} and the end of the pIWP and IWC increase, respectively. Data have been smoothed out using 6-h running average.

Table 1: Pearson linear correlation coefficient *R*, regression coefficient *α* (mg m^{-3} mm^{-1} h) and the offset *β* (mg m^{-3}) from the correlation between precipitation and Ice Water Content (IWC), and Water Vapour (WV) in the upper troposphere (UT, at 146 hPa), at Day, Night and Day−Night over the 7 tropical zones and the average over the 6 zones (μ_{6Zones}).

930

		Land			Ocean				
		SouthAm	SouthAfr	MariCont-L	IndOc	PacOc	MariCont-O	MariCont	μ_{6Zones}
IWC	$R\ (IWC^{UT}_{Day}, P_{Day})$	0.7	0.8	0.5	0.8	0.8	0.6	0.5	0.7
	$\alpha\ (IWC^{UT}_{Day}, P_{Day})$	8.1	15	9.3	4.8	5.9	7.5	8.9	8.4
	$\beta\ (IWC^{UT}_{Day}, P_{Day})$	0.9	0.0	1.1	0.3	0.4	0.7	1.0	0.6
	$R\ (IWC^{UT}_{Night}, P_{Night})$	0.7	0.7	0.6	0.9	0.7	0.6	0.6	0.7
	$\alpha\ (IWC^{UT}_{Night}, P_{Night})$	4.8	6.1	5.6	4.7	6.8	7.7	5.4	5.9
	$\beta\ (IWC^{UT}_{Night}, P_{Night})$	0.6	0.6	1.4	0.3	0.2	0.6	1.6	0.6
	$R\ (IWC^{UT}_{Day\text{-}Night}, P_{Day\text{-}Night})$	0.6	0.7	0.7	0.1	0.2	0.5	0.5	0.5
WV	$R\ (WV^{UT}_{Day}, P_{Day})$	0.4	0.3	0.2	0.0	0.3	0.1	0.2	0.2
	$\alpha\ (WV^{UT}_{Day}, P_{Day})$	0.0	0.0	0.0	0.0	0.0	0.0	0.0	0.0
	$R\ (WV^{UT}_{Night}, P_{Night})$	0.5	0.5	0.1	0.0	0.5	0.0	0.0	0.3
	$\alpha\ (WV^{UT}_{Night}, P_{Night})$	0.0	0.0	0.0	0.0	0.0	0.0	0.0	0.0
	$R\ (WV^{UT}_{Day\text{-}Night}, P_{Day\text{-}Night})$	-0.0	-0.1	0.2	0.2	0.0	0.1	0.2	0.1

935

940

Table 2: Differences between the amount of Ice Water Content (IWC) estimated from TRMM and MLS injected in the upper troposphere (UT) and the tropopause layer (TL) (*ΔIWC^{UT}* and *ΔIWC^{TL}*, respectively), and partial Ice Water Path (pIWP) measured by SMILES in the UT (*ΔpIWP_{SMILES}*) and IWC measured by SMILES in the TL (*ΔIWC_{SMILES}*), during the period DJF 2009-2010, and their differences (*ΔIWC^{UT}-ΔpIWP_{SMILES}* and *ΔIWC^{TL}-ΔIWC_{SMILES}*, in the UT and the TL, respectively). The average over the land and ocean zones (*μ(Lands ZonesTropics)*, *μ(Oceans ZonesTropics)*, respectively) are also presented.

		UT			TL		
		ΔIWC^{UT} (mg m^{-3})	$\Delta pIWP_{SMILES}$ (mg m^{-3})	$\Delta IWC^{UT}-\Delta pIWP_{SMILES}$ (mg m^{-3})	ΔIWC^{TL} (mg m^{-3})	ΔIWC_{SMILES} (mg m^{-3})	$\Delta IWC^{TL}-\Delta IWC_{SMILES}$ (mg m^{-3})
L A N D	SouthAm	2.1	2.8	-0.7	0.34	0.29	+0.05
	SouthAfr	1.5	1.8	-0.3	0.23	0.27	-0.04
	MariCont-L	2.5	2.3	+0.2	0.35	0.23	+0.12
O C E A N	IndOc	1.1	1.0	+0.1	0.34	0.09	+0.15
	PacOc	1.0	1.6	-0.5	0.21	0.24	-0.03
	MariCont-O	0.5	1.0	-0.6	0.10	0.08	+0.02
	μ(Lands ZonesTropics)	2.1	2.3	- 0.3	0.31	0.26	+0.05
	μ(Oceans ZonesTropics)	1.2	1.2	+0.0	0.22	0.13	+0.09

Table 3: Time of the onset of the ice injection in the tropical upper troposphere (UT), (t_{on}^{UT}), duration of the injection of ice in the UT (Δt^{UT}), minimum amount of ice in the UT (IWC_{min}^{UT}), and amount of ice injected into the UT (ΔIWC^{UT}) as a function of the 6 study zones and averaged over the land and ocean zones (μ(Lands ZonesTropics), μ(Oceans ZonesTropics), respectively) during DJF from 2004 to 2017. The bolded values highlight the most important injection of ice and the associated regions.

Region	t^{UT}_{on} (LT)	Δt^{UT} (h)	IWC^{UT}_{on} (mg m^{-3})	ΔIWC^{UT} (mg m^{-3})
SouthAm	08:00-09:00	7	1.6	2.0
SouthAfr	08:00-09:00	7	1.3	2.9
MariCont-L	08:00-09:00	8	1.0	**3.3**
IndOc	17:00-18:00	9	1.0	0.4
PacOc	17:00-18:00	9	1.5	0.5
MariCont-O	17:00-18:00	11	1.6	**0.9**
μ(Lands ZonesTropics)	08:00-09:00	7	1.3	2.7
μ(Oceans ZonesTropics)	17:00-18:00	10	1.4	0.6

Table 4: As a function of the delay (δt = 0, 1, 2, or 3 h) between the beginning of the Prec onset and the IWC onset in the tropical tropopause layer (TL): duration of the injection of ice in the TL $\left(\Delta t^{TL}\right)$, minimum amount of ice in the TL $\left(IWC^{TL}_{min}\right)$ and amount of ice injected into the TL $\left(\Delta IWC^{TL}\right)$ as a function of the 6 study zones and averaged over the land and ocean zones (μ(Lands ZonesTropics), μ(Oceans ZonesTropics), respectively) during DJF from 2004 to 2017. The bolded values highlight the most important IWC^{TL}_{min} and ΔIWC^{TL} and the associated regions.

Zones	δt = 0 h			δt = 1 h			δt = 2 h			δt = 3 h		
	Δt^{TL} (h)	IWC^{TL}_{min} (mg m^{-3})	ΔIWC^{TL} (mg m^{-3})	Δt^{TL} (h)	IWC^{TL}_{min} (mg m^{-3})	ΔIWC^{TL} (mg m^{-3})	Δt^{TL} (h)	IWC^{TL}_{min} (mg m^{-3})	ΔIWC^{TL} (mg m^{-3})	Δt^{TL} (h)	IWC^{TL}_{min} (mg m^{-3})	ΔIWC^{TL} (mg m^{-3})
SouthAm	7	0.22	0.26	6	0.23	0.25	5	0.28	0.20	4	0.35	0.13
SouthAfr	7	0.19	0.40	6	0.21	0.38	5	0.26	0.33	4	0.35	0.24
MariCont-L	8	0.17	**0.56**	7	0.19	**0.55**	6	0.23	**0.50**	5	0.32	**0.42**
IndOc	9	0.24	0.10	8	0.24	0.10	7	0.25	0.09	6	0.26	0.09
PacOc	9	0.29	0.09	8	0.29	0.09	7	0.29	0.09	6	0.30	0.08
MariCont-O	11	**0.34**	**0.19**	10	**0.35**	**0.18**	9	**0.36**	**0.17**	8	**0.37**	**0.16**
μ(Lands ZonesTropics)	7	0.19	0.41	6	0.21	0.39	5	0.26	0.34	4	0.34	0.26
μ(Oceans ZonesTropics)	10	0.29	0.13	9	0.29	0.12	8	0.30	0.12	7	0.31	0.11

Table 5: Difference *d* between Ice Water Content measured by MLS during the decreasing phase (*IWC$_x$*) and Ice Water Content estimated at the same hour (*IWC(x)*) in the upper troposphere (UT) and the tropopause layer (TL), (where *x* = Day or Night as a function of the timing of the decreasing phase of the ice diurnal cycle).

	Zones	*d* in the UT (mg.m^{-3})	*d* in the TL (mg.m^{-3})
L	SouthAm	+0.48 (+ 23 %)	-0.08 (- 20 %)
A **N**	SouthAfr	+0.44 (+ 20 %)	-0.07 (- 18 %)
D	MariCont-L	-0.09 (- 3 %)	-0.09 (- 14 %)
O	IndOc	0.17 (- 21%)	-0.02 (- 7 %)
C **E**	PacOc	-0.20 (- 10 %)	+0.03 (+ 9 %)
A **N**	MariCont-O	-0.47 (- 26 %)	-0.04 (- 8 %)

Appendix 1: List of Abbreviations and Acronyms and Their Meanings

Acronyms	Meanings
CPT	Cold Point Tropopause
DJF	December, January, February
IndOc	Indian Ocean
IWC	Ice Water Content
LS	Lower Stratosphere
LT	Local Time
MariCont	Maritime Continent
MariCont-L	Maritime Continent land
MariCont-O	Maritime Continent ocean
MLS	Microwave Limb Sounder
Prec	Precipitation
pIWP	partial Ice Water Path
PacOc	Pacific Ocean
RHI	Relative Humidity with respect to Ice
SouthAm	South America
SouthAfr	South Africa
TEMP	Temperature
TL	Tropopause Layer
TRMM	Tropical Rain Measuring Mission
TST	Tropophere to Stratosphere Transport
TTL	Tropical Tropopause Layer
UT	Upper Troposphere
WV	Water Vapour

1015

1020